AN ABSTRACT OF THE THESIS OF

Victor Emerald Hauser, Jr. for the Doctor of Philosophy in
(Name) (Degree)

Chemical Engineering.
(Major)

Date thesis is presented Aug. 6, 1963

Title: A STUDY OF CARBON ANODE POLARIZATION IN FUSED CARBONATE FUEL CELLS

Redacted for Privacy

Abstract Approved: _____

The graphite anode reaction in a fused carbonate electrolyte is studied theoretically and experimentally. Data on open circuit cell potentials indicate, for operation below 900°C, only a small fraction of the free energy of reaction is converted to electrical work.

Anode polarization measurements were made for current densities of up to 77.5 ma/cm^2 for several temperatures between 600°C and 940°C. Initial polarization is shown to be capacitive in nature and accounts for up to 75 percent of the anode polarization. The double layer charge capacitance is 308 $\pm$ 15 microfarads per square centimeter at 600°C.

A number of chemical analyses of the anode reaction product gases are made for current densities from 13.7 ma/cm^2 to 141 ma/cm^2 and for temperatures from 650°C to 870°C. High concentrations of carbon dioxide in the reaction product gas, combined with measured gas evolution rates for various cell currents, show that the

main cell reaction corresponds to one which results in the oxidation of carbon electrochemically to carbon dioxide. The presence of carbon monoxide, at all temperatures investigated, indicates that the anode reaction is a multistep process which includes the production of carbon monoxide as an intermediate species.

A STUDY OF CARBON ANODE POLARIZATION IN FUSED CARBONATE FUEL CELLS

by

VICTOR EMERALD HAUSER, JR.

A THESIS

submitted to

OREGON STATE UNIVERSITY

in partial fulfillment of
the requirements for the
degree of

DOCTOR OF PHILOSOPHY

June 1964

APPROVED:

Redacted for Privacy

(Associate Professor of Chemical Engineering)

Redacted for Privacy

(Head of Department of Chemical Engineering)

Redacted for Privacy

(Dean of Graduate School)

Date; Aug. 6, 1963

Typed by Joan Shaw

ACKNOWLEDGMENTS

The author wishes to express his gratitude to Professor R. E. Meredith for his valued help and encouragement; and to Professors R. E. Gaskell and J. J. Brady for their review of this thesis.

I am indebted to my friend Mr. Michael J. Schaer who has offered suggestions and helpful criticisms during the course of this work.

Grateful acknowledgments are also given to Dow Chemical Co., Texaco Oil Co., and to the Electrochemistry Society for generous financial supports.

Finally, the author wishes to extend a very special thanks to his wife, Carolyn, for her understanding and encouragement, especially during the conclusion of this work.

TABLE OF CONTENTS

A STUDY OF CARBON ANODE POLARIZATION IN FUSED CARBONATE FUEL CELLS

I. INTRODUCTION

At present the bulk of the energy production in the world is derived from the chemical bonds in coal, petroleum, and natural gas; but in the process of converting this chemical energy into work most of the available energy is lost. The generation of electrical energy from such fossil fuels, in general, involves the combustion of the fuel to create heat which is converted to mechanical energy by a heat engine. The mechanical energy, in turn, is used to drive a generator rotor to produce useful electrical energy. This series of events is carried out in modern central power stations with energy conversion efficiencies close to 30 percent. The major reason for this low energy conversion is the theoretical limitation of the temperature dependent Carnot efficiency that applies to all heat engines. This fundamental energy loss usually amounts to over 80 percent for practical heat engines. However, in contrast to the use of a heat engine in the electrical power production cycle, the galvanic cell offers a means of converting chemical energy directly to electrical energy with theoretical efficiencies approaching 100 percent.

The galvanic cell used for such energy conversion has been called for many years, a fuel cell, and it differs from a battery in two major aspects: First, in principle it is able to operate

continuously as long as fuel and air are supplied to the cell and, second, the fuel is usually a carbonaceous compound or a derivative of a carbonaceous compound. Hydrogen, commonly obtained from natural gas, is one derivative that is extensively used as a fuel in power producing cells.

The first voltaic pile and the modern dry cell of today are fuel cells in a sense; they convert chemical energy directly into electricity and succeed in doing so with very high efficiencies. Use, however, is made of expensive fuels such as zinc, lead, and mercury and if the energy originally required to refine such metals were included in the energy balance, this overall conversion efficiency from chemical to electrical energy would be much less than that obtainable in modern steam generating plants.

Because the galvanic or fuel cell has such a high potential for converting the chemical energy of common fuels into electrical energy, the development of a workable system has attracted the attention of investigators for many years. Grove (13) described an experiment as early as 1839 that showed electrical energy could be produced by the electrochemical oxidation of hydrogen by oxygen. This oxidation was carried out in a galvanic cell that had dilute sulfuric acid as the electrolyte, and platinum foil as the electrodes.

Although fuel cells share the common background of electrochemical oxidation of the fuel that is supplied to them, they can be

divided arbitrarily into two main classifications: the direct type and the indirect type. "Direct" fuel cells might be defined as those in which carbonaceous material such as coke or natural gas are oxidized at the anode, and "indirect" cells make use of gaseous fuels such as carbon monoxide and hydrogen, usually produced by some chemical means from an original carbonaceous material.

Additional breakdowns in fuel cell classification are commonly made on the basis of temperature. The low temperature cells are those which operate between room temperature and 100°C. Medium temperature cells, or intermediate temperature cells, operate from 100°C to approximately 400°C, and the high temperature cells operate in the range between 400°C and 1000°C or higher.

Much progress has been made in recent years in the development of devices that achieve useful current densities. Most of it has been made with systems that operate in the temperature range between 20°C and 250°C and are of the indirect fuel cell type. The most common reactants utilized in these cells are hydrogen and carbon monoxide fuels and oxygen or air. The well known water gas reaction is a useful means of producing such fuels. It may be written as

$$C + H_2O \xrightarrow[\text{heat}]{} CO + H_2. \qquad (1)$$

The gases that are produced in the water gas reaction can then be

fed directly into the cell which will anodically oxidize the hydrogen and carbon monoxide to form water vapor and carbon dioxide.

Before an economical unit can be produced, many problems must be surmounted. To understand some of the problems involved, let us consider a gaseous hydrogen-oxygen system: It is common knowledge that hydrogen and oxygen combine to produce water, for the elements existing separately possess more energy than the water molecules. However, at ordinary temperatures and pressure, the elements coexist indefinitely since additional activation energy must be supplied to raise the molecules to such an energy state that they might combine chemically. Heating the gas to about 500^{o}C provides the necessary activation energy, and the reaction then procedes spontaneously producing large quantities of heat.

The hydrogen-oxygen fuel cell accomplishes essentially the same reaction by several steps, each of which has a particular activation energy. Instead of only producing heat as in direct combustion, electrode processes can be devised whereby electrochemical reactions are possible which force electrons through an external circuit from the anode to the cathode. This flow of electrons through some external circuit can be made to do electrical work.

It has been the goal of all investigators in the field of fuel cells to carry out the electrochemical reactions at high rates and with little energy loss in the form of heat. It is axiomatic, however, that

the more rapid the electrochemical reaction is carried out, the lower the cell voltage becomes, and the greater is the proportion of chemical energy that is converted directly to heat. In this case considerable chemical energy is expended in the activation step of the electrochemical reaction, and it becomes the function of an electrochemical catalyst to lower the energy barriers, thus permitting high electrode reaction rates with a minimum loss in cell voltage and heat. In addition to losses due to activation energy barriers, energy is required to pump or move the reactants and products through the system, which further reduces the efficiency of a practical cell.

There are other important problems which must be considered, which can be solved only through intensive developmental work, such as the power output per unit volume at high thermodynamic efficiency and the length of time a cell can operate before it deteriorates.

Statement of the Problem

In this dissertation we investigate the characteristics of the electrochemical reaction occurring at a graphite anode immersed in a fused alkali carbonate electrolyte. Primarily we are concerned with the determination of the anode potential over a wide range of current density and operating temperature. In order to carry out such polarization measurements, suitable means of containing the corrosive carbonate melt and of supporting the electrodes in the

high temperature environment have to be developed. In addition, direct measurement of the anode polarization requires the use of non-polarizing reference electrodes, and consideration must be given to the uncertain behavior of such electrodes in the molten electrolyte. Also of major importance in this study is the experimental determination of what electrochemical reactions occur at the graphite electrode for various temperatures and current densities. In order to determine which reactions occur, means have to be developed to sample, analyze and measure evolution rates of the gaseous products of the anode reaction.

The Model and Variables

In reviewing the published work on this subject, one finds many specific fuel cells with their performance frequently tabulated as a function of temperature and current density. It is unfortunate, however, that almost invariably the performance data applies only to the overall cell and it is almost impossible to assign any shortcomings observed in the cell behavior to any particular component. In addition, it was common to add certain depolarizers in hopes of obtaining desirable results, but, more often than not, this rendered the problem of analyzing the actual electrode process more difficult.

To make the present problem more conducive to an analysis, a simple crucible type cell was constructed with the electrodes dipping

directly into a free electrolyte. This was done to eliminate the common problem of poor electrode to electrolyte contact usually found in electrolyte systems employing an inert solid matrix to retain what would be a molten or fused electrolyte. Associated with such bound electrolytes is also the problem of installing reference electrodes in a fixed and known relationship to the electrodes. The system variables that are fixed or set are: the oxidizing gas composition, electrolyte composition, temperature of cell operation, and current flow through the cell. Observed variables are mainly anode polarization and anode reaction product composition.

For the purposes of this work, anode polarization will be defined as the difference in the initial potential and the final potential as measured between the anode and the anode reference electrode before and during current flow through the cell. respectively.

II. PREVIOUS WORK

As recent as 1945, most attempts to construct satisfactory fuel cells were highly empirical in nature and are presently only of historical significance. Detailed reviews of early work have been written by several authors of which the more significant are by Baur and Tobler (5), 1933, and H. C. Howards (15), 1945. Reviews of the more recent developments are presented by the following authors: McKee and Adams (25), 1949; Adams (1), 1954; and Justi, Bischoff, and Spengler (22), 1956.

The present day field of fuel cell research and development is broad and varied. Because of this, the review for this dissertation will be, for the most part, confined to work done on carbon-oxygen cells in fused salt electrolytes with emphasis on the alkali carbonate electrolytes.

The Work of Haber and Bruner-1904

Haber and Bruner investigated the high temperature fuel cell using carbon as the anode and iron, contacted with air, as the cathode (14). The electrodes, immersed in fused alkali, were shown to behave as an oxygen-hydrogen cell due to the presence of active hydrogen generated by the chemical reaction between carbon and the hydroxyl ions in the melt. Although carbon was consumed in the cell

reaction, the electrolyte was also irreversibly decomposed, which resulted in subsequent cell degradation. The following reaction was said to occur in the cell:

$$2Fe_2O_3 + C + 2NaOH \rightleftharpoons Na_2CO_3 + H_2O + 4FeO. \quad (2)$$

The Work of Taitelbaum-1910

This investigator studied carbon and iron electrodes immersed in fused sodium hydroxide as in the study by Haber and Bruner (30). The effect of various additives to the electrolyte were determined, and the addition of manganese dioxide seemed beneficial in the maintenance of the cathode potential. The addition of hydrogen, sawdust, hydrocarbons, and carbon monoxide to the carbon anode compartment permitted current densities up to 0.5 ma/cm^2 at 50 percent cell polarization. Cell operating temperatures were between 370°C to 390°C.

The Work of Baur and Ehrenburgh-1912

In 1912 Baur and Ehrenburgh published details of their work on carbon-oxygen cells which employed a variety of electrolytes including sodium tetraborate, cryolite and aluminum oxide mixtures, sodium potassium silicates with a potassium fluoride additive, and potassium sodium carbonate mixtures (2). A novel molten silver

cathode was used which had the decided advantage of limiting the required electrode-electrolyte interfacial contact to two phases. Oxygen was soluble in the molten silver and could be supplied for the cathodic reaction simply by bubbling air into the silver. Data on overall cell voltages were given for several currents. Unfortunately, electrode areas were not stated for the fused carbonate experiments, making comparison to data reported in this dissertation impossible. For the fused cryolite-alumina electrolyte the authors stated that open circuit potentials were 1.02 volts and that a current density of 50 ma/cm^2 could be obtained at 20 percent polarization of the overall cell at $1000^{o}C$. Examination of the data, however, reveals that an error of more than an order of magnitude was made, in that, for 20 percent polarization a current of only 40 milliamps was passed through a carbon electrode with 19 square centimeters of surface area. The correct current density would be 2.2 ma/cm^2 for the above conditions of 20 percent polarization, or 0.80 volts output, at $1000^{o}C$.

The Work of Baur, Petersen, and Füllemann-1916

These authors report that cell potentials were determined for carbon in combination with cathodes of copper oxide and lead oxide (3). The electrolyte employed was fused borax. Open circuit potentials were measured over the temperature range of $950^{o}C$ to $1300^{o}C$

and varied from 0.6 volts to 1.1 volts for the lead oxide cathode and from 1.12 volts to 1.4 volts for the copper oxide cathode. By considering the free energy of various reactions and correcting for the known decomposition pressure of the oxide cathodes, it was shown that the open circuit potentials corresponded to the reaction

$$2\,C + O_2 = 2CO. \qquad (3)$$

The Work of Baur, Treadwell, and Trümpler-1921

These authors studied a cell consisting of a carbon anode, a magnetite-ferric oxide cathode and a magnesium oxide separator impregnated with fused sodium carbonate and potassium carbonate (6). At 800°C the open circuit potential was 1.04 volts and at 40 percent polarization of the overall cell potential the current density was 7.3 ma/cm^2. The impregnation of the diaphram with the fused salt provided good electrolytic conduction, yet did not wet the cathode. The non-wetting of the cathode allowed good oxygen transport to the reacting surface, but the electrolyte-electrode interfacial contact area was limited. No data were offered indicating the cathode's contribution to the cell polarization.

In a later work of E. Baur and co-workers (4) the suggestion was made to use a solid, electrolytically conducting separator between the carbon anode and iron oxide cathode. This necessarily required high temperatures in order to achieve a low internal cell

resistance and reduce the polarization due to internal resistance. An electrolyte, claimed to have optimum properties, consisted of 8.35 mole percent CeO_2, 8.35 mole percent Li_2ZrO_3, 33.30 mole percent clay, and 50.00 mole percent WO_3. The cell resistance at 1100°C was about one ohm between the electrodes and circuit voltages varied from 0.6 to 0.7 volts. Current densities could not be determined from the description of the system, but the best cell produced 0.77 watts per liter at a cell potential of 90% of open circuit.

The Work of Tamaru and Kamada-1935

In a study of the carbon-oxygen fuel cell, Tamaru determined that carbon dioxide was the only anode reaction product at 700°C (31). The conditions for this determination were not completely stated since only the total current and not the current density was given. The stoichiometry was determined by comparing the measured loss of the anode mass to the calculated loss for various assumed anode reactions, by measuring the volume of gas, and by analyzing the gas evolved from the anode. The measured mass loss was 93 percent of theoretical for the reaction

$$C + O_2 = CO_2 \qquad (4)$$

and the analysis of the gas sample, collected from the anode

reaction, yielded 92 percent carbon dioxide and eight percent nitrogen. The electrolyte used in the 400°C to 550°C range was a potassium, sodium, and lithium carbonate eutectic mixture of unspecified composition. The 550°C to 600°C range was investigated with mixtures of sodium-lithium carbonates and alkali halides.

Using separate reference electrodes, experiments were also conducted in order to determine the individual electrode polarization values. These measurements were claimed to have shown that polarization occurred at both electrodes at 400°C to 500°C, but from 550°C to 600°C the polarization occurred mainly at the oxygen electrode. Unfortunately no polarization data were presented and no quantitative estimate may be made as to the value of the anode polarization, either as a function of current density or of temperature, beyond the above qualitative remarks.

III. EXPERIMENTAL PROCEDURE AND DATA ON ANODE POLARIZATION

The Need for the Study of Anode Polarization

Prior to the design of any practical fuel cell an extensive knowledge of the behavior of both the anode and cathode should be known for all operating conditions and electrode reaction rates. Such information concerning the kinetics of carbon anodes in fused carbonates is notably lacking, since virtually all work reported considered the overall cell voltage at various current densities. This method of reporting cell performance leaves open to question which electrode and to what degree is each electrode responsible for the irreversible behavior.

Work by Douglas (33, p. 129) employed reference electrodes in fused carbonate cells with carbon monoxide or hydrogen as fuel and air or oxygen as the cathodic gas. Information about the oxygen electrode behavior obtained from this work, in conjunction with cell ohmic drop and overall cell performance data of the carbon-oxygen fuel cell could, in principle, yield carbon anode polarization data. The cathode construction, electrolytes, and cell operating temperatures, however, are significantly different from those described in the literature and the calculated anode polarizations would have little value. It is the primary purpose of this present study to obtain, in a

direct manner, carbon anode polarization data over a wide range of operating temperatures and current densities.

Selection of the Electrolyte and Electrode Materials

If we are to obtain electrical energy from the reaction

$$C + O_2 = CO_2 \qquad (4)$$

by the electrochemical reaction of carbon and oxygen, these elements must be present at the electrodes of the cell. In order to have the electrochemical cell reaction proceed, each element must acquire a charge either by sending ions into the electrolyte or by discharging ions from the electrolyte. Since carbon is believed not to ionize under ordinary conditions, and oxygen does so only slowly, the only apparent possibility of obtaining reasonable reactivity from such a system is to appeal to high temperatures.

To achieve high temperatures it becomes necessary to use either molten salt or solid electrolytes, since the vapor pressure of ordinary aqueous systems would be prohibitively high. The free molten salt system was chosen because of the good electrode-electrolyte contact it offered and the ease of locating a reference electrode in such a system. In selecting a particular salt for the electrolyte, it was determined from the outset that no additives or "depolarizers" were to be added and only a species whose function was necessary

to the cell operation and which was stable at all operating temperatures would be chosen. For these reasons all alkali halides, sulfates, nitrates, and hydroxides were eliminated since no plausible mechanisms involving these salts could be predicted which had the necessary overall effect of leaving the electrolyte unchanged by the cell reaction. Use of fused nitrates had been shown by Bacquerel (7) to result in a nitrite-nitrate couple because of the chemical reduction by carbon. The use of fused hydroxides also offered a similar objection since Haber (14) showed that the carbon electrode, in fact, acted as a hydrogen electrode due again to the chemical decomposition of the electrolyte. Fused alkali carbonates were therefore chosen since they alone seemed to satisfy all the above criteria.

To extend the useful temperature range of operation of the fused carbonate, a eutectic mixture with a melting point of 403°C was used in all experiments. The eutectic composition in mole percent was 40 percent lithium carbonate, 30 percent potassium carbonate, and 30 percent sodium carbonate.

The selection of the electrode materials for the cell presented little choice once the fused carbonate had been chosen for the electrolyte. Because of the extreme corrosiveness of fused carbonates, it was found that high temperature alloys of stainless steel and inconel were chemically attacked and contaminated the electrolyte. Only metals such as gold, platinum, and palladium were found to

resist such attack. After considerable experimentation with the construction of porous silver electrodes the project was abandoned and a simple bubbling gas electrode, constructed of 80 percent gold and 20 percent palladium was used as the oxygen-carbon dioxide cathode. Purified dense graphite was chosen as the anode material in order to avoid, as much as possible, unknown electrochemical catalytic effects, that might be exhibited by any one of a number of impurities present in all electric arc carbons or formed carbon rods.

The 80 percent gold, 20 percent palladium alloy used in the cathode and crucible construction proved very satisfactory in that, after the equivalent of more than three months operation, no observable chemical attack occurred. An additional benefit in the use of the gold alloy was that it formed a high melting solution (1250°C) which permitted the welding together of cell components with the lower melting pure gold wire (melting point-1064°C), provided great care was taken to avoid overheating and melting the alloy.

Method of Obtaining Data on Electrode Polarization

Technique and design factors

The equipment and procedure used to obtain data on the anodic overvoltage was designed with the following points in mind: The overall cell performance, though of some interest, was not the object of this study and attempts to achieve high current density with the cell

acting in a spontaneous manner were not undertaken. There were several reasons for this action but the most important was the inability to construct good cathode structures of porous noble metals having a satisfactory and uniform pore size.

It is extremely important for good cathode operation to have uniform pore size in porous metal gas electrodes. If nonuniform sized pores exist, the pressurized gas behind such a porous structure would bubble through into the electrolyte at a large pore while the fused salt electrolyte would penetrate the small pores by capillary action and flood the electrode in that area. However, the technology required to construct satisfactory gas diffusion electrodes for fused carbonate operation was not available to the author.

Also necessary to high cell performance is low internal cell resistance. The usual way of reducing this resistance is to increase the area of conductance through the electrolyte and to decrease the distance between the electrodes. This was not done in this work in order to simplify cell construction and to allow adequate clearance between electrodes for the positioning of reference electrodes.

In lieu of cathodes capable of high current density, it was decided to construct a simple cylindrical cathode, 5.1 centimeters high and one centimeter in diameter, from an 80 percent gold-palladium sheet, 0.004 inches thick. Oxygen was introduced near the bottom of the cylinder positioned along the electrode axis as illustrated

in Fig. 1. Louvers were cut in the electrode sides to allow good contact between the electrolyte, electrode, and rising gas bubbles, and at the same time prevent the escape of gas bubbles into the electrolyte between the electrodes.

A rather serious consequence of the direct introduction of gas into the electrolyte at the cathode, was the formation of bubbles on the surface of the electrolyte which produced considerable spattering of the liquid when the bubbles broke. This spattering thoroughly wetted all cell components mounted above the electrolytes in early experiments and resulted in electrode shorting and gradual loss of electrolyte. Control of bubble spatter was achieved by cutting a row of louvers in the cathode above the electrolyte liquid level. This served to vent the gas and liquid, which welled up from inside the cathode, in a downward direction to burst the bubbles before they could grow large (refer to Fig. 1).

Use of such a simple cathode system has the immediate disadvantage of complete polarization at rather small cathodic current densities. The consequence of such easy polarization is that high current densities at the anode may not be achieved unless either the anode surface is much smaller than that of the cathode, or an external power source is used to drive the cell reaction at a higher rate than would occur in spontaneous operation. Of course, driving the cell reaction with an external power source can result in

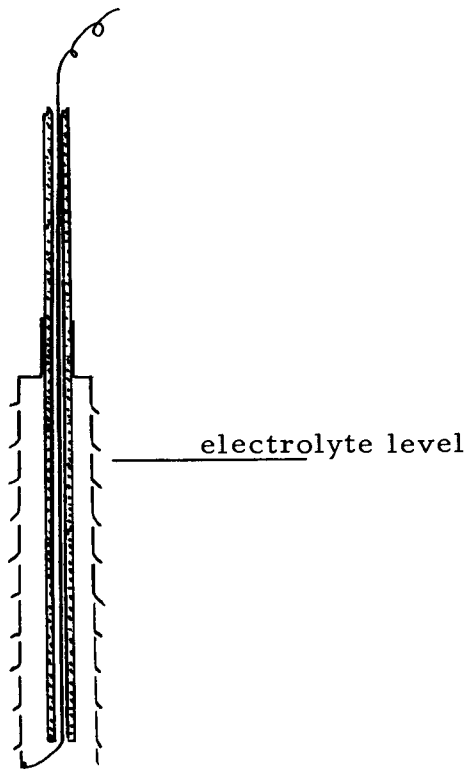

Fig. 1. Drawing (to scale) of the working cathode.

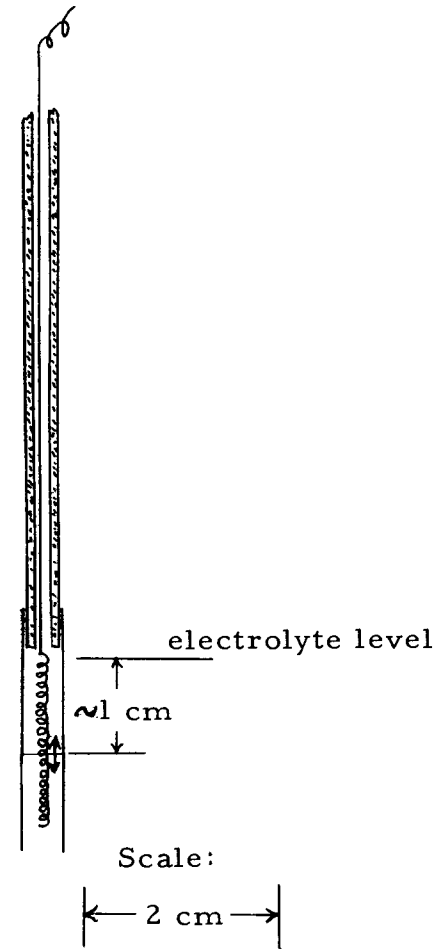

Fig. 2. Drawing (to scale) of the anode gas reference electrode.

abnormal electrode processes. Such reactions, in this case, are confined to the cathode provided complete polarization of the anode is not achieved.

The graphite rod which served as the anode was mounted parallel to the cathode by pushing a heavy platinum wire into a tight fitting hole drilled in the center of the anode. The cell was operated with the graphite electrode completely submerged except for a narrow neck of graphite extending through the electrolyte interface. This narrow graphite neck protected the platinum wire from anodic dissolution.

Alongside the anode were mounted two reference electrodes; one was a graphite cylinder, slightly smaller in diameter than the anode, the other was a platinum wire coiled inside, but not contacting, a gold-palladium tube into which gas could be introduced (see Fig. 2). Provision was made to feed gas of the same composition, which had been introduced at the cathode, into this second reference electrode under carefully controlled pressure. It was necessary to insure positive gas pressure inside the gold alloy tube and at the same time prevent excess pressure from forcing gas out the bottom of the reference electrode in order to eliminate voltage fluctuations due to intermittant contact of the electrode with the electrolyte. In addition to maintaining a controlled gas pressure, in what will henceforth be termed the gas reference electrode, it was desirable

to superimpose small rapid oscillations in the gas pressure to cause the electrolyte to alternately wash the wire surface inside the metal tube. This provided a continuous replenishing of the oxygen and carbon dioxide in the electrolyte surrounding the reference electrode wire. Both objectives of controlling pressure and pulsing the pressure were accomplished, as shown in Fig. 5, by the dip tube located in the gas supply line to the gas reference electrode. The hydrostatic pressure of water above the bottom of the dip tube determined the gas pressure to the reference electrode, and the slow bubbling of excess gas through the water provided adequate pressure variation in the reference electrode system.

Of fundamental importance to cell operation and meaningful measurements was the prevention of electrical short circuits between the electrical leads leaving the cell. To prevent such electrical failures due to either high temperature breakdown by semiconduction, or to electrical conduction by parts unavoidably wetted, even slightly, during cell operation, it was found necessary to use recrystallized alumina for both the electrode supports and the spacer-crucible cover above the electrolyte. Electrode leakage resistance was checked at operating temperatures before and after each run by removing the electrode assembly from the electrolyte. The interelectrode resistance was found to be greater than 200,000 ohms after successful runs.

To avoid chemical attack on electrical leads from the cell and to eliminate any question regarding possible thermal emf generated in the system only platinum wires were used in the cell, and all dissimilar metal connections were made in the same high temperature region inside the cell.

Equipment

The electrode assembly and cell crucible required for the study of anode polarization are shown in Fig. 3. The apparatus shown consisted of:

1) An 8.4 centimeter high, 4.4 centimeter inside diameter alumina crucible. *
2) An 80 percent gold, 20 percent palladium crucible liner made of metal rolled to a thickness of 0.004 inches. The liner's function was to contain the fused carbonate while the alumina crucible supported the liner at high temperatures.
3) A reference electrode of platinum wire coiled inside a gold-palladium metal tube mounted above the electrolyte on a recrystallized alumina tube. The electrolyte entered the tube bottom and was pulsed up and down over the coiled

* No. 528 - 903, Laboratory Equipment Corp., St. Joseph, Michigan.

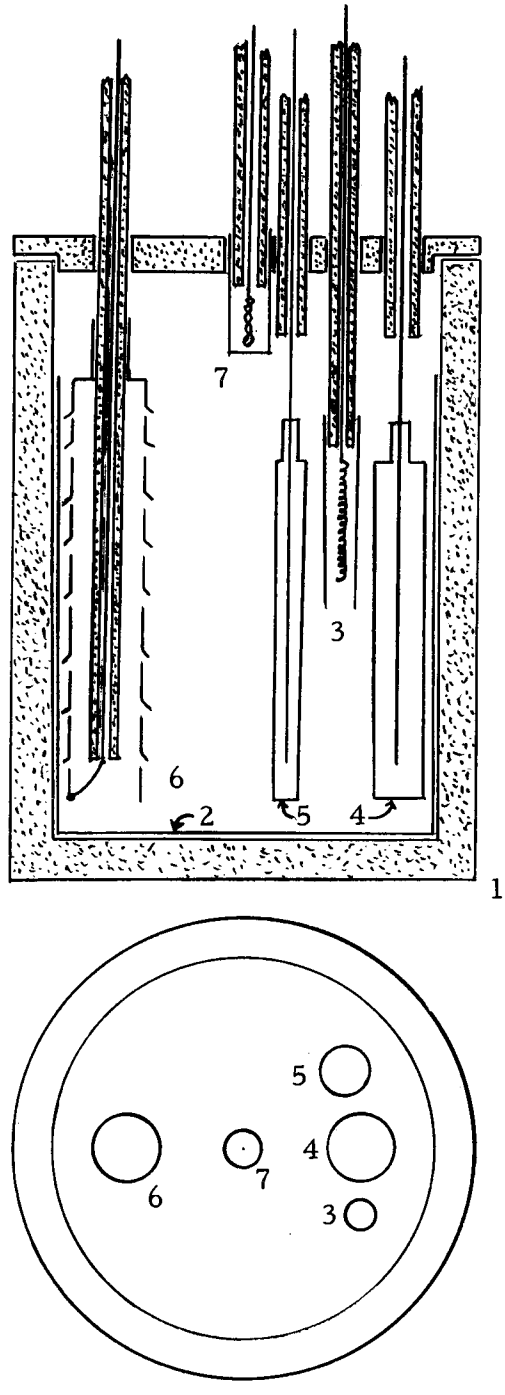

Fig. 3. Schematic drawing of electrode assembly and crucible.

platinum wire section by a pulsating gas pressure inside the tube.

4) A high grade dense graphite anode[#] supported on a platinum mounting wire. The mounting wire was forced into a tight fitting drilled hole and served as both an electrode holder and current collector for the anode.

5) A graphite reference electrode similar to the working anode.

6) A louvered 80 percent gold, 20 percent palladium cathode cylinder with an alumina gas induction tube in the center. The electrode connection wire is led up through the inside of the gas supply tube.

7) A type K chromel-alumel thermocouple [*] used for both temperature control and temperature indication. For protection against chemical attack, the thermocouple is enclosed in a gold alloy capsule.

In addition to the cell assembly a tube furnace fitted with a protective stainless steel liner was used to heat the system to a maximum of 1000°C. The furnace temperature was controlled with a Honeywell Pyr-O-Volt proportional controller which employed a magnetic amplifier and saturable core reactor to control the power

---

No. P 7206, Grade AVC, National Carbon Co., San Francisco, California.

* Model No. 9A1K3 Wire, S. O. R2-116147-3 and S. O. R2-116147-2, Minneapolis - Honeywell Regular Co., Philadelphia 44, Pa.

input to the furnace. Control was attained to within 2°C. The temperature controller was checked periodically for temperature calibration with a Leeds and Northrup K-2 potentiometer. Thermocouple calibration was checked at 100°C (boiling water) and at 960°C (melting point of silver). Temperatures as indicated on the Honeywell controller were used in the tabulated data. An ice bath reference junction was used at all times.

Since the cell impedance normally changes during discharge, a fixed resistance load across a cell generally results in both the cell voltage and the discharge current changing with time. To overcome this difficulty and to bring about the discharge of the cell under more controlled conditions, a simple constant current source (or sink depending on magnitude of current flow) was constructed. Current control was achieved by connecting a large variable resistance in series with a 48 volt lead acid battery.

The cell control panel wiring diagram is shown in Fig. 4 and the components are:

1) A 0-100 milliammeter. *
2) A 0-1000 milliammeter. *
3) Two 24 volt aircraft storage batteries.
4) A 0-10,000 ohm variable resistance to regulate the current through the cell.

* Model 420, Triplett Electrical Instrument Co., Bluffington, Ohio.

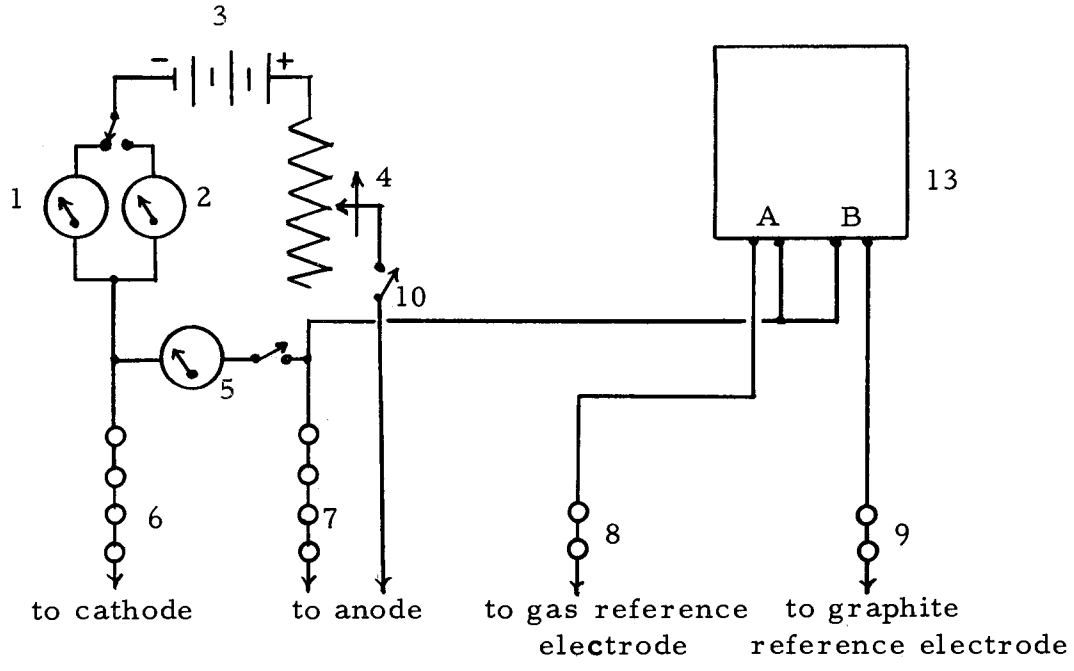

Fig. 4. Electrical circuit for anode polarization measurements.

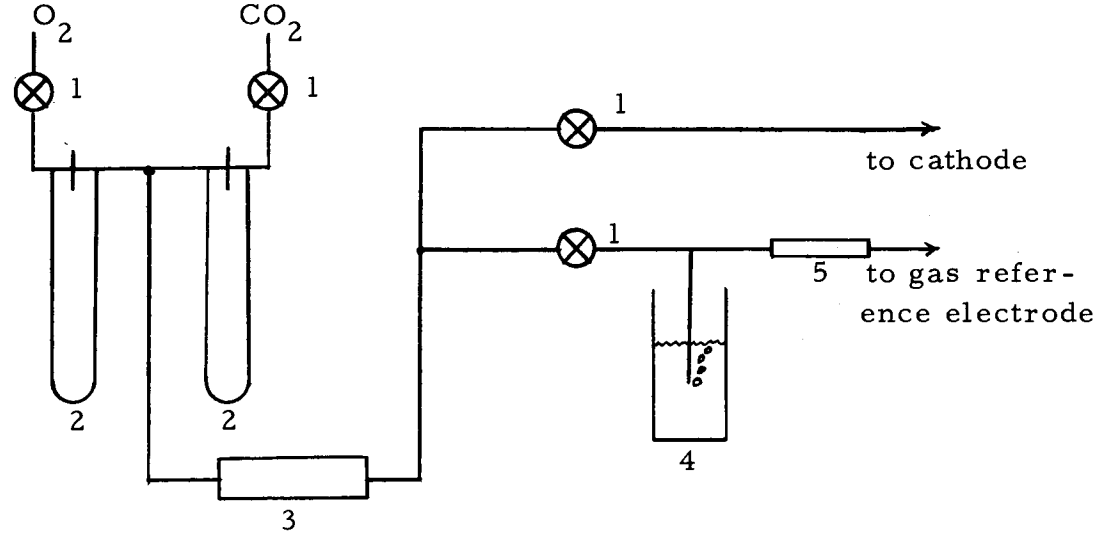

Fig. 5. Schematic diagram of gas supply system for cathode and gas reference electrode.

6, 7, 8, 9) Tipjacks connected in parallel as shown to provide multiple electrical connections to the cell cathode, anode, gas reference, and graphite reference, respectively. A separate wire conducts the cell current to the anode to eliminate potential drop in the anode measuring circuit due to resistance losses.

10) A switch to control current flow through the cell.

11) A switch in series with two tipjack receptacles. Opening this switch and inserting a shunt resistance across it provided a means of obtaining a voltage proportional to cell current which was useful as an input to a recorder.

12) A S. P. D. T. switch for selecting either the high or low range milliammeter.

13) A two channel strip chart recorder # with an input impedance of 100,000 ohms on the 0-1 volt scale and 200,000 ohms on the two volt range. Channel A measures the anode polarization by means of the gas reference electrode and channel B by means of the graphite reference electrode.

The cathode and gas reference electrode oxygen and carbon dioxide metering and pressure control system is shown in Fig. 5. The components are:

1) Gas control needle valves. *

---

* No. 116, The Matheson Co., Newark, California.

Servo-riter Recorder - Texas Instruments Inc., Houston, Texas.

2) Manometer and orifice gas flow meters. The orifices were made by drawing ten millimeter glass tubes down to filaments which were mounted within another glass tube for protection. The flow meter system was calibrated to within three percent over the range of 1.3×10^{-2} to two ml/sec.

3) A calcium chloride drying tube - ten inches long by one inch diameter.

4) A pressure regulator for the gas reference electrode which operated at a pressure determined by the hydrostatic head over the bottom of the dip tube. A second purpose of the regulator was to set up small oscillations in gas pressure to improve the gas electrolyte-electrode contact in the gas reference electrode.

5) A calcium chloride drying tube to prevent accidental induction of water into the operating cell and to eliminate the possibility of significant amounts of water vapor diffusing from the water bubbler into the reference electrode supply line.

An overall view of the laboratory equipment used in these experiments in shown in Fig. 6.

Experimental Procedure

The dry mixed electrolyte consisting of 40 percent lithium

Fig. 6. A view of the equipment used in the anode polarization study.

carbonate, 30 percent potassium carbonate and 30 percent sodium carbonate (in mole percent) was packed in the cell crucible, placed in the furnace and heated to 800°C to completely fuse the mixture. Several subsequent additions of powdered electrolyte mixture to the melt were needed to bring the liquid level to a point where the electrolyte would just cover the anode. About 76 milliliters of electrolyte were required. After the electrolyte was completely fused, the temperature was lowered to about 600 °C so the preheated electrode assembly could be lowered into the furnace with a minimum of thermal stress on the ceramic parts.

Immediately after installation of the electrodes in the cell, a dry mixture of 50 percent carbon dioxide and 50 percent oxygen was bubbled into the melt through the cathode gas induction tube and introduced into the reference electrode under a controlled pressure of one-half inch of water. The cathode gas bubbling rate was set at about 0.20 milliliters per second and allowed to bubble several hours before cell operation to insure that water absorbed during storage and handling would be swept out of the system. This gas bubbling rate was maintained at all times during the experiment. If by accident the gas supply was shut off, both the cathode and gas reference induction tubes would become completely plugged within five minutes. This was due to the fact that at equilibrium the partial pressure of carbon dioxide over the melt is about 0.1 millimeters at 750°C and

the absorption of the relatively concentrated carbon dioxide in the induction tube created a partial vacuum in the tube. This partial vacuum then allowed the melt to rise inside the tube until it contacted a cooler region where it inconveniently solidified.

Before each experiment, the furnace temperature controller was set to the desired temperature, and the cell was allowed to remain at that temperature for at least one hour before a polarization run was made. Polarization data were obtained by a simultaneous recording, on a two channel recorder, of the difference in potential between each of the reference electrodes and anode as a function of time. The recorder was started before the run and the change in polarization, when an electrical load was applied to the cell, was recorded. Because of the relatively slow response time of the electromechanical recording system, some runs were made using an oscilloscope-camera combination to determine the true initial change in polarization with time.

The data were always taken first by going from high to low currents, then, to check the first run, data were collected for increasing currents. The cell was allowed to reach a constant open circuit reference to anode potential before the next run at a different current density was made. Usually only three to five minutes were required to obtain constancy of the open circuit reference potentials although, at the high temperatures, from ten to 15 minutes were

required for high current densities.

A Note Regarding Accuracy

The random error introduced in the current and temperature measurements is essentially independent of the conditions of the run. Both are limited to the accuracy of the interpolation of the scale increments. No noticable drift could be detected in either the milliammeter or temperature reading during a run. It would be possible to determine the temperature more accurately with a K-2 potentiometer, but the temperature controller sensitivity could only be adjusted to achieve control to within $\pm$ 2°C, which is the limit for visual detection of the temperature indicator needle movement. The milliammeters could be read to within one percent of full scale reading.

Systematic errors present in polarization measurements are dependent upon the conditions of the run. At low current densities the polarization potential becomes the same order of magnitude as cell voltage variations due to the bubbling of gas through the cathode. At the other extreme, at high current densities, a systematic error can occur as a consequence of a cathodic reaction rate which exceeds the limiting current density for oxygen discharge. The resulting decomposition of the electrolyte produces transient concentrations of Na_2, K_2, and Li_2 oxides that might have adverse effects on the reference electrode potentials. Further comment on this problem will be

presented in the discussion section of this experiment.

Polarization potentials recorded on the two channel strip chart recorder can be determined to within five millivolts. The recorder was checked periodically during each experiment for both zero and full scale voltage calibration. No observable drift was noticed after warm up of the recorder. Although the recorder used was potentiometric, the external attenuation circuit had an input impedance of 100,000 ohms for the zero to one volt scale and 200,000 ohms for the zero to two volt scale. Experiments conducted on the current carrying capacity of the reference wire electrodes showed that 0.01 milliamps resulted in a reference electrode polarization of less than two millivolts at 640°C (see Appendix). No permanent polarization of the reference electrodes could be detected for such low currents.

Results and Conclusions

The polarization or voltage drop at the anode is tabulated in Tables I through VI as a function of anode current density for the several specified temperatures. These measurements are also plotted in Figs. 7 and 8. Data plotted in Fig. 8 indicated the reproducibility of measurements for two runs made 24 hours apart.

The overpotential measurements for the runs with decreasing current densities ($i\downarrow$) and increasing current densities ($i\uparrow$) are given in tabulated form. No identification between run up and run down

Table I. Polarization Data for the Graphite Anode at 600°C.

Anode area: 7.77 cm^2

Open circuit potential: 0.55 volts

$CO_2 = O_2$: 0.145 ml/sec

$i\downarrow$ (ma/cm^2)	η (volts)	$i\uparrow$ (ma/cm^2)	η (volts)
36.4	0.546	0.93	0.252
30.5	0.520	3.54	0.351
20.6	0.498	6.25	0.394
12.4	0.454	8.90	0.420
8.88	0.420	11.3	0.440
6.30	0.400	17.4	0.474
3.99	0.362	24.3	0.505
2.99	0.319	38.2	0.545
1.35	0.279		
0.799	0.238		
0.645	0.225		

Table II. Polarization Data for the Graphite Anode at 700°C.

Anode area: 7.77 cm^2

Open circuit potential: 0.69 volts

$CO_2 = O_2$: 0.145 ml/sec

$i\downarrow$ (ma/cm^2)	η (volts)	$i\uparrow$ (ma/cm^2)	η (volts)
69.5	0.588	1.05	0.193
56.6	0.571	3.09	0.294
47.5	0.560	8.94	0.400
38.4	0.542	12.5	0.432
26.8	0.512	20.3	0.480
18.5	0.476	30.6	0.515
12.5	0.438	41.2	0.542
8.95	0.400	51.5	0.563
6.30	0.367	62.3	0.584
3.09	0.302	70.5	0.596
1.57	0.230		
0.72	0.152		

Table III. Polarization Data for the Graphite Anode at 700°C. *

Anode area: 7.77 cm^2

Open circuit potential: 0.69 volts

$CO_2 = O_2$: 0.145 ml/sec

$i\downarrow$ (ma/cm^2)	η (volts)	$i\uparrow$ (ma/cm^2)	η (volts)
74.7	0.608	1.87	0.254
60.3	0.583	3.61	0.318
51.5	0.565	8.05	0.397
33.6	0.526	12.4	0.440
18.0	0.470	30.1	0.520
12.9	0.448	46.4	0.561
8.05	0.400	62.0	0.584
5.74	0.365	75.4	0.605
2.58	0.290		
1.03	0.194		

* This table represents data taken under identical conditions as the data for Table II for the purpose of showing reproducibility.

Table IV. Polarization Data for the Graphite Anode at 800°C.

Anode area: 7.77 cm^2

Open circuit potential: 0.82 volts

$CO_2 = O_2$: 0.145 ml/sec

$i\downarrow$ (ma/cm^2)	η (volts)	$i\uparrow$ (ma/cm^2)	η (volts)
71.4	0.562	1.22	0.138
62.6	0.548	2.68	0.214
48.8	0.520	4.57	0.260
36.9	0.494	7.90	0.320
31.3	0.478	11.4	0.363
15.7	0.390	18.1	0.411
12.6	0.366	27.8	0.465
9.00	0.328	44.6	0.516
6.37	0.291	52.2	0.530
3.09	0.228	67.2	0.555
1.59	0.157	74.2	0.564
0.79	0.100		

Table V. Polarization Data for the Graphite Anode at 880°C.

Anode area: 7.77 cm^2

Open circuit potential: 0.93 volts

$CO_2 = O_2$: 0.145 ml/sec

$i\downarrow$ (ma/cm^2)	η (volts)	$i\uparrow$ (ma/cm^2)	η (volts)
74.4	0.520	4.83	0.198
53.4	0.492	8.68	0.256
39.3	0.421	12.0	0.290
31.3	0.387	19.0	0.342
15.7	0.327	34.8	0.412
12.0	0.291	47.5	0.457
7.65	0.244	62.5	0.487
4.84	0.197	73.0	0.515
1.93	0.119		

Table VI. Polarization Data for the Graphite Anode at 940°C.

Anode area: 7.77 cm^2

Open circuit potential: 1.01 volts

$CO_2 = O_2$: 0.145 ml/sec

$i\downarrow$ (ma/cm^2)	η (volts)	$i\uparrow$ (ma/cm^2)	η (volts)
77.5	0.498	1.29	0.053
62.0	0.472	5.69	0.160
44.0	0.425	11.1	0.221
27.8	0.360	22.0	0.320
14.8	0.271	44.0	0.410
11.4	0.238	56.2	0.445
6.05	0.172	63.7	0.465
2.58	0.102	76.4	0.490
0.902	0.040		

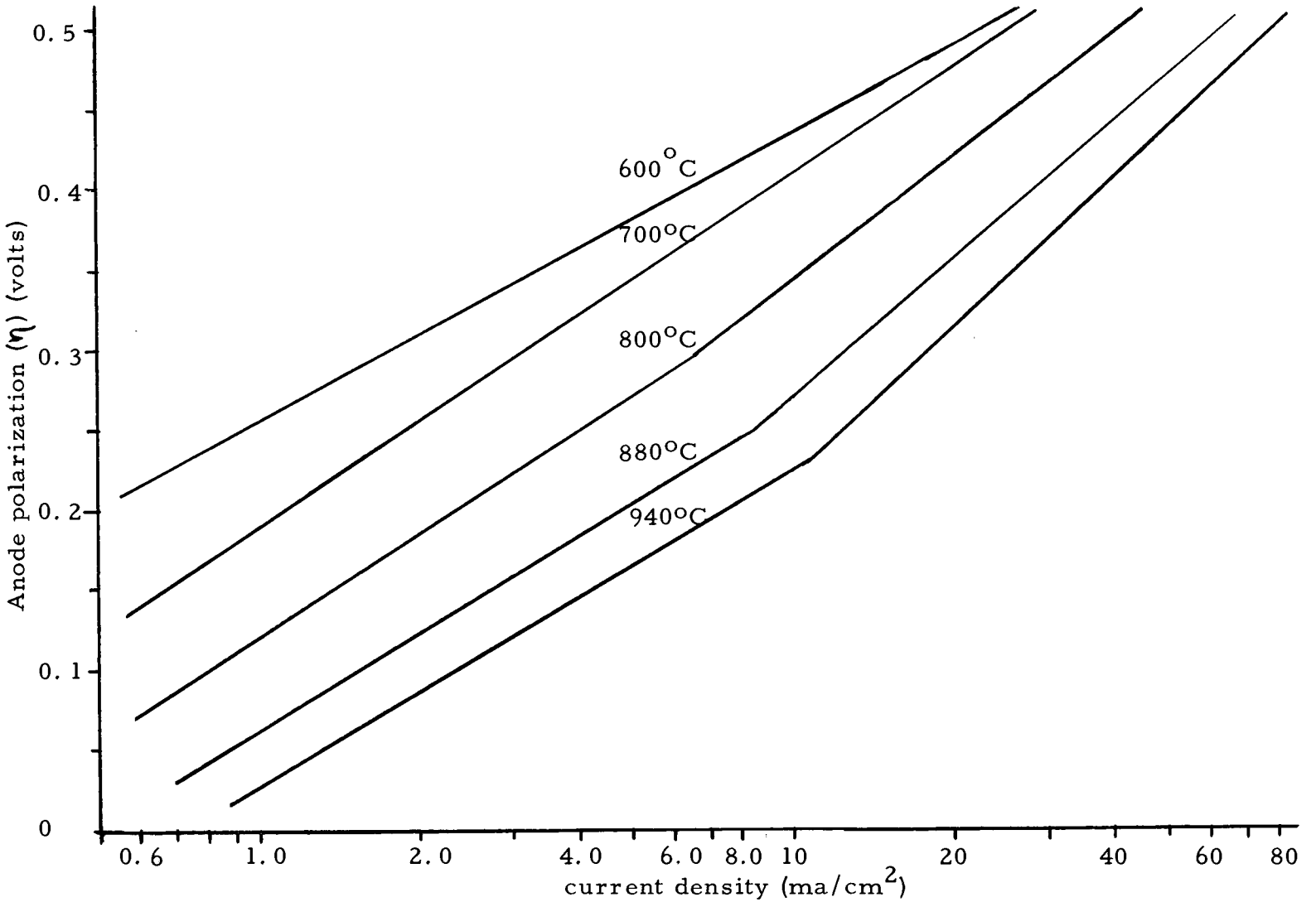

Fig. 7. Graphite anode polarization measurements.

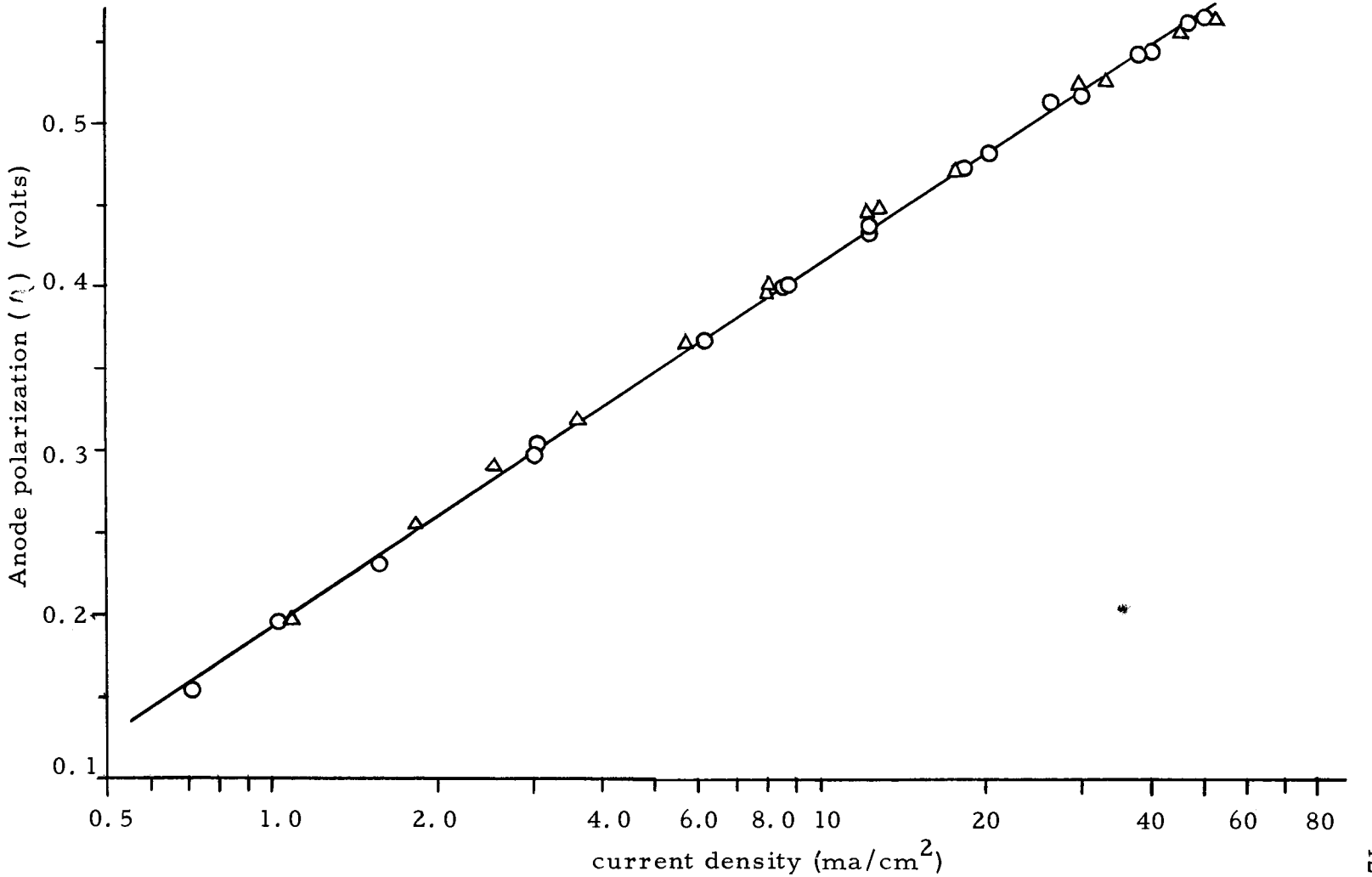

Fig. 8. Reproducibility of anode polarization data at 700°C.

data, plotted in Figures 7 and 8, was made since no trend was distinguishable.

All polarization measurements tabulated in Tables I through VI are with respect to the gas reference electrode, as are the open circuit potentials listed. Open circuit measurements between the working cathode and the gas reference agreed to within 15 millivolts for a fresh cathode before cell operation at high current densities. Immediately after operation at high current densities, the gas reference to cathode potentials were as high as -1.18 volts which decayed to -0.2 volts in about ten minutes. It is possible that the high initial negative potential is due to sodium, lithium, or potassium metal, or to carbon monoxide formation at the cathode. The latter material as well as carbon was found to form at the cathode, but a discussion of this will be postponed until Chapter V.

Although all reported polarization measurements are with respect to the gas reference electrode, simultaneous recording of the potential differences between the gas reference electrode and anode, and graphite reference and anode, were made on the two channel recorder. Without exception, the potential change with respect to each reference electrode was identical to within two millivolts for current densities less than 14 ma/cm^2. At high current densities (75 ma/cm^2) the anode polarization measured at the graphite reference electrode was always high by about ten millivolts. Similarly, the potential

measurement between the two reference electrodes was found to vary by the same two to ten millivolts when the cell load was switched on. Oscilloscope traces were obtained for the gas reference to graphite reference potential when the cell was loaded, and rise times for the reference electrode "polarization" were less than one millisecond. It is believed this polarization is due to the location of the two reference electrodes at different potentials in an electric field induced in the electrolyte during current flow between the working electrodes. It was encouraging to note that observed variations in open circuit potentials between the gas reference and anode, particularly after high current density runs, were also observed in the graphite reference potential. The open circuit reference potentials were sometimes 30 to 40 millivolts higher after a series of high current density runs. Since both types of reference electrodes registered the same increase in potential, it is concluded that processes occurring at the anode are solely responsible for any increase in the open circuit potential and reaction products building up in the electrolyte are not significantly affecting the reference electrodes themselves. It seems plausible that the transient high open circuit anode potential is due to a build up of carbon monoxide on the graphite anode from the electrochemical reaction that had just taken place. More will be said about this phenomenon in Chapter V.

As is apparent after examination of Fig. 7, the polarization data appear to fit an empirical equation first established by Tafel,

$$* \quad \eta = a \ln i + b \qquad (5)$$

Some theoretical justification for the fitting of polarization data to a logarithmetic expression, such as the Tafel equation, might be made if it can be assumed that the velocity of the rate determining reaction is controlled by some electrically charged reactant having at least energy, U, and obeys a Maxwellian energy distribution. Recognition that the rate of reaction is increased when the anode is made more positive leads to the conclusion that the electric field at the electrode surface affects the rate controlling reaction energy. If the anode potential is E, it is reasonable to assume the electric field in the electrolyte only partially affects a reactive charged species, since the electric field due to the charged electrode extends out several molecular diameters into the electrolyte. The incoming particle, although gaining energy from the electric field, can give up some of this energy by colliding with particles near the electrode, thus assuming some of the energy properties of the paricles within the electric field. If β is the fraction of the electric field effectively acting on the reactive species, the energy of the reactive species is increased by an amount $\beta \, \overline{E} \cdot \overline{d}$, where $\overline{E}$ is the electric field and $\overline{d}$

---

* For convenience all symbols are tabulated in Nomenclature. Wherever possible, standard notation has been used.

is the path traveled along the field. The total energy barrier for an electrochemical reaction is then $U - \beta \overline{E} \cdot \overline{d} n F$, where U is the energy of activation at zero electrode to solution potential difference, n is the charge of the reacting ion, and F is Faraday's constant. Applying the law of mass action to the rate equation, the velocity of the reaction must be proportional to the activity (a_A) of the reacting species. Hence:

$$i = kFa_A e^{-\frac{U - \beta \overline{E} \cdot \overline{d} n F}{RT}}, \qquad (6)$$

where k is a proportionality constant. The exponential factor arises from the Maxwellian energy distribution assumption and expresses the fraction of the reactive species, A, having the energy required to initiate the electrochemical reaction.

Since the energy induced into the charged active species A by the electric field along the path $\overline{d}$ is due to the difference in potential between the electrode and bulk electrolyte and hence is proportional to the polarization η, we may write:

$$\beta \overline{E} \cdot \overline{d} = \alpha \eta . \qquad (7)$$

Substituting (7) into (6) and solving for η we obtain:

$$\eta = \frac{RT}{\alpha nF} \ln i - \frac{RT}{\alpha nF} \ln (kFa_A) + \frac{U}{\alpha nF} \qquad (8)$$

which is of the same form as the Tafel equation (5).

It should be pointed out that the derivation is not valid for very low current densities, as the limiting condition of

$$\lim_{i \to 0} \eta = 0 \qquad (9)$$

is clearly not achieved by Eq. (8), although this is a necessary limiting condition. This, of course, is due to neglecting the reverse electrochemical reaction at the anode in the derivation, which becomes significant at low discharge rates.

According to equation (8), the slope of a Tafel line is

$$\left(\frac{\partial \eta}{\partial \ln i}\right)_T = \left(\frac{RT}{\alpha n F}\right) \qquad (10)$$

provided the change in α and U with respect to a change in current may be neglected.

Analysis of the Tafel plots of Fig. 7 show a distinct change in slope at about eight ma/cm^2 for the higher operating temperatures. This slope change indicates a change in the reaction mechanism, but, in the light of present results, it is not possible to further elucidate upon why this occurs.

The values of the product αn are calculated from Eq. (10) for both high and low current density regions for various temperatures and are listed in Table VII.

The value of n in Eq. (8) corresponds to the number of charges on the active species, which until now has not been identified. If the reactive species is carbonate ion then the anode reaction is

$$1/2\ C + CO_3^{=} = 3/2\ CO_2 + 2e \qquad (11)$$

Table VII. Tafel Slopes for Several Temperatures.

Current density less than 6 ma/cm^2			Current density greater than 13 ma/cm^2	
Temperature °C	$\left(\frac{\partial \eta}{\partial \ln i}\right)_T$ volts	αn	$\left(\frac{\partial \eta}{\partial \ln i}\right)_T$ volts	αn
600	0.0785	0.950	0.0785	0.950
700	0.0955	0.872	0.0955	0.872
800	0.0938	0.980	0.113	0.814
880	0.0872	1.13	0.123	0.808
940	0.0955	1.09	0.136	0.764

and n equals two. If the transfer coefficient α is taken to be 0.5, as is commonly done when more information is lacking [see Janz and Colen (18, p. 6)], it is seen that calculated values for n vary between 2.18 and 1.42.

Information regarding the activation energy U may be obtained by differentiation of Eq. (8) with respect to temperature at constant current. If the variation of U and α with temperature can be neglected, the expression

$$\left(\frac{\partial \eta}{\partial T}\right)_i \qquad \frac{\alpha nF\eta - U}{T\alpha nF} \tag{12}$$

may be obtained. For low current densities the assumption with respect to the dependence of U and upon temperature is more acceptable than at high current densities, since errors tend to

cancel due to the relative constancy of the ratio $(\frac{U}{\alpha nF})$ at low current densities.

Smoothed polarization data from Fig. 7 is plotted in Fig. 9 for current densities of one,, six, and 20 ma/cm^2. Slopes at 600^o and 800^{o}C were determined graphically from Fig. 8 and activation energies were calculated with the aid of Eq. (12). These results are given in Table VIII.

Activation energy values listed in Table VIII show a rather large change with current density and temperature. It is believed this scatter in U is due, for the most part, to an inadequate number of polarization runs at different temperatures. Such heavy reliance on only five widely spaced temperature runs can result in considerable error in the polarization temperature coefficient and hence in the activation energy. Also of importance in the activation energy determination is the possible effect of the change in reaction mechanism as evidenced in the change in slope of the Tafel lines in Fig. 7. The change in slope occurs in the higher temperature runs as the current density approaches about ten ma/cm^2. The convergence of the lines for the 600^{o}C and 700^{o}C runs near 50 ma/cm^2 indicates that the polarization is becoming independent of temperatures, thus it is seen in Eq. (12) that the activation energy, U, approaches the value of αnF (13 Kcal/mol). It is concluded the activation energy can be estimated only as 18 $\pm$ 5 Kcal/mole and a more intensive study must

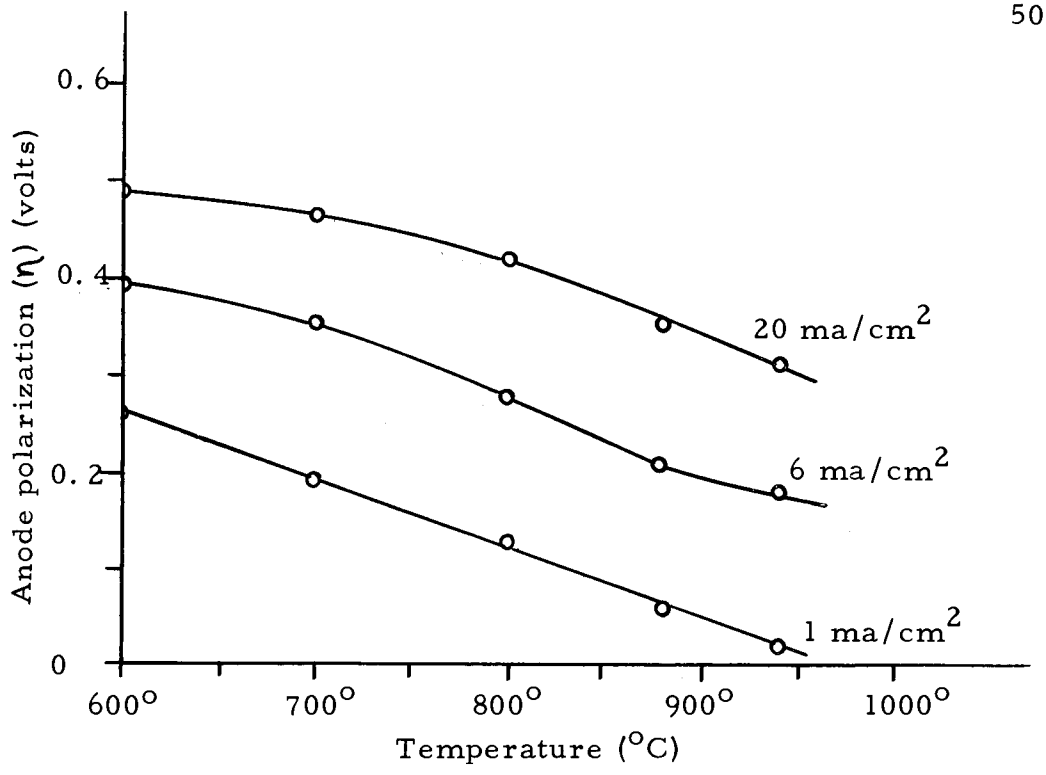

Fig. 9. Anode polarization variation with temperature.

Table VIII. Activation Energy of the Anode Reaction.

	T = 600°C		T = 800°C	
i	$(\frac{\partial \eta}{\partial T})_i$	U	$(\frac{\partial \eta}{\partial T})_i$	U
ma/cm^2	m. v. /°C.	Kcal/mol	m. v. /°C	Kcal/mol
1	-0. 675	18. 4	-0. 675	19. 0
6	-0. 245	12. 2	-0. 875	28. 9
20	-0. 100	12. 3	-0. 670	21. 1

be made of the graphite anode polarization before a more accurate calculation is possible.

In addition to the steady state polarization data already discussed, measurements of the changing anode potential during the initial phases of discharge were made. Polarization-time data obtained by photographing an oscilloscope trace and values obtained from the photograph traces are listed in Table IX.

Table IX. Transient Anode Polarization Data.

Temperature: 600°C
Anode area: 7.7 cm^2

$i = 84.3\ ma/cm^2$		$i = 8.37\ ma/cm^2$		$i = 0.707\ ma/cm^2$	
t (milli-seconds)	(volts)	t (milli-seconds)	(volts)	t (milli-seconds)	(volts)
0.30	0.080	1.6	0.045	5.6	0.015
0.40	0.110	3.4	0.088	16.0	0.040
0.50	0.152	4.6	0.128	26.0	0.058
0.70	0.220	6.0	0.156	36.0	0.077
0.90	0.264	7.5	0.184	46.0	0.085
1.2	0.336	12.5	0.240	56.0	0.098
1.8	0.410	20.0	0.282	76.0	0.118
2.8	0.460	30.0	0.310		
5.0	0.480	40.0	0.320		

A plot of the polarization as a function of time for the three current densities in Table IX is given in Fig. 10. The initial variation in polarization is seen to be linear in time, which is suggestive of a capacitive type discharge of the double layer at the anode. The equation for such a capacitive discharge is

$$C = \frac{idt}{d\eta} \tag{13}$$

Initial values of $\left(\frac{\partial \eta}{\partial t}\right)_i$ for the three curves of Fig. 10 are listed in Table X together with the apparent capacity calculated for each current from Eq. (13).

Table X. Capacity of Anode During the Initial Stages of Polarization at 600°C.

Anode area: 7.77 cm^2		
(i ma/cm^2)	$\left(\frac{\partial \eta}{\partial t}\right)_i$ (volts/millisecond)	C $\frac{(\text{microfarads})}{cm^2}$
84.3	0.290	291
8.37	2.59 (10^{-2})	323
0.707	2.23 (10^{-3})	317

The average value of the electrode capacitance at 600°C is taken as 308 microfarads/cm^2. Higher temperature data indicate this electrode capacitance is 370 $\frac{\text{microfarads}}{cm^2}$ at 800°C and 590 $\frac{\text{microfarads}}{cm^2}$ at 880°C.

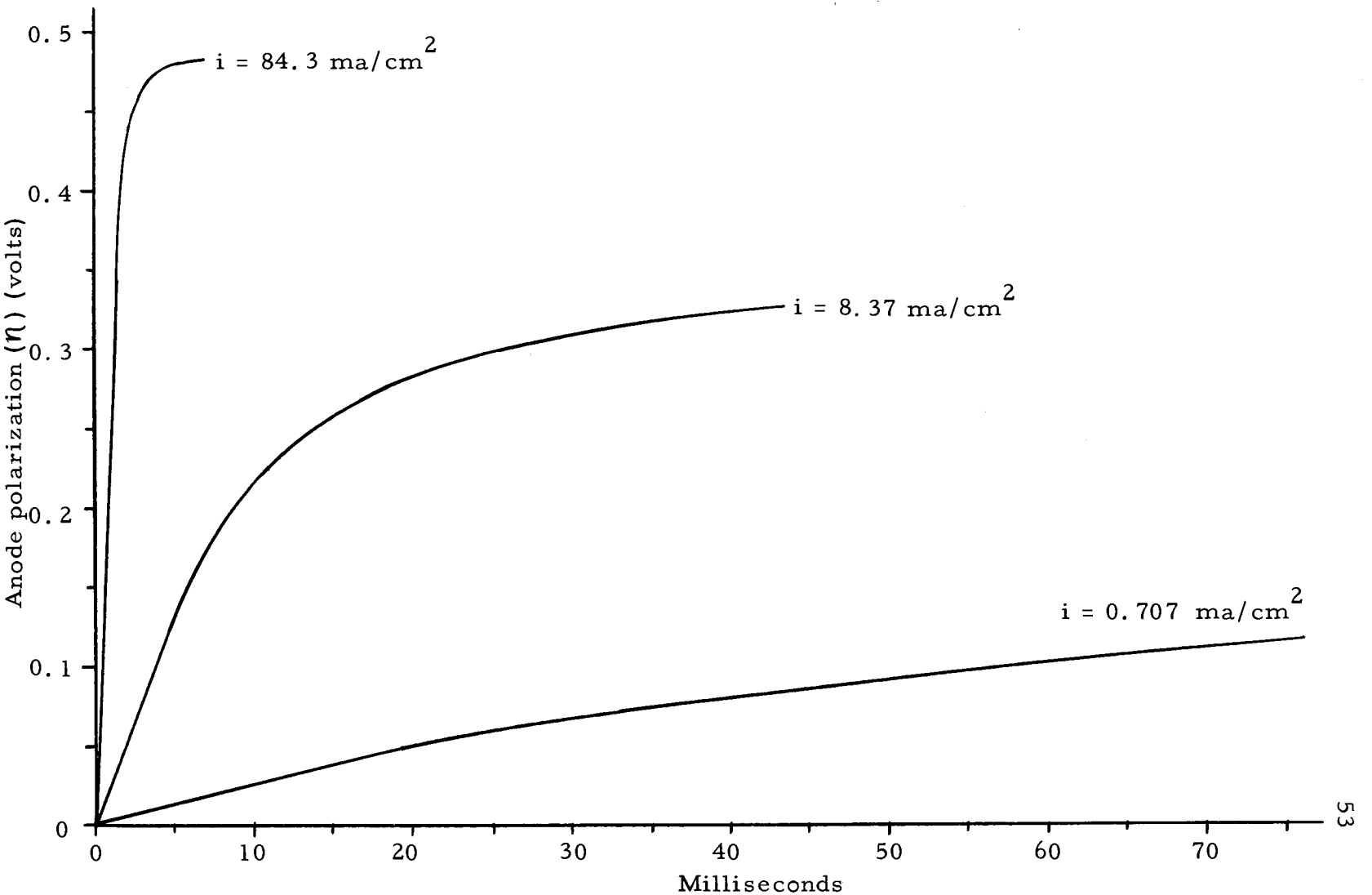

Fig. 10. Transient anode polarization measurements at 600°C.

The small variation in capacity calculated for the three current density values in Table X demonstrates that the anode polarization is due principally to discharge (or charging) of a Stern double layer. It is not clear whether a double layer is being formed or being discharged during the initial polarization of the anode.

One Model would have alkali ions, M^+, oriented adjacent to the graphite anode interface and distributed in a more diffuse manner further from the electrode for the open circuit configuration. During polarization the anode becomes less electronegative, thus it becomes unable to maintain the high concentration of M^+ ions near anode surface. The M^+ ions leaving the vicinity of the anode constitute a current flow though no ions are discharged at the anode interface during the initial phase of polarization. Not until the anode becomes sufficiently electropositive does an electrochemical reaction occur at a sufficient rate at the anode for the potential to stabilize at some lower value.

An alternate initial polarization mechanism might be the charging, rather than the discharging, of a double layer described above. If the state of the electrolyte near the electrode can be considered identical to that of the bulk electrolyte for the open circuit condition, a net movement of the electronegative constituent ($CO_3^=$) in the electrolyte towards the anode would occur during the initial moments of cell discharge. The $CO_3^=$ ions arriving at the solution side of

the developing double layer do not discharge to any marked extent at first, and a condenser type of charging behavior for the initial phase of the anode polarization is the result.

The anode potential curves of Fig. 10 are nonlinear with respect to time after polarization of about 50 percent of the steady state value is reached. This nonlinear portion of the curve represents a complicated series of events occurring at the anode. Among these are concentration polarization with respect to the anodic reactants and reaction products, and blocking of active regions of the anode surface by gas bubble formation. The final phase of the anode polarization becomes linear with respect to time again with up to five seconds required for a steady state value to be established. This latter phase is most probably due to the steady growth of gas bubbles on the anode surface, which start breaking off and rising to the electrolyte surface when steady state polarization is reached.

IV. EXPERIMENTS ON THE REVERSIBILITY OF THE ANODE REACTION

The Need for the Study

Data have been obtained on the open circuit potentials for the carbon-oxygen cell in the course of the experiments on anode polarization described in the preceeding chapter. The potential of the graphite electrode, as measured with respect to the gas reference electrode, lies considerably below the theoretical potentials of various possible electrode reactions employing carbon and oxygen as reactants.

The purpose of this experiment is to determine if the anode reaction behavior in the neighborhood of zero current flow corresponds to that of a reversible electrode and whether thermodynamic considerations are valid in the theoretical treatment of the various possible anode reactions.

Equipment

The cell and electrode assembly shown schematically in Fig.11 is identical to that used in the polarization experiments. The external electrical circuit was modified from that of the previous experiment by the substitution of the potentiometer and battery package for the constant current source. A shunt resistance was added to the circuit to provide a voltage input for the x-y recorder that was

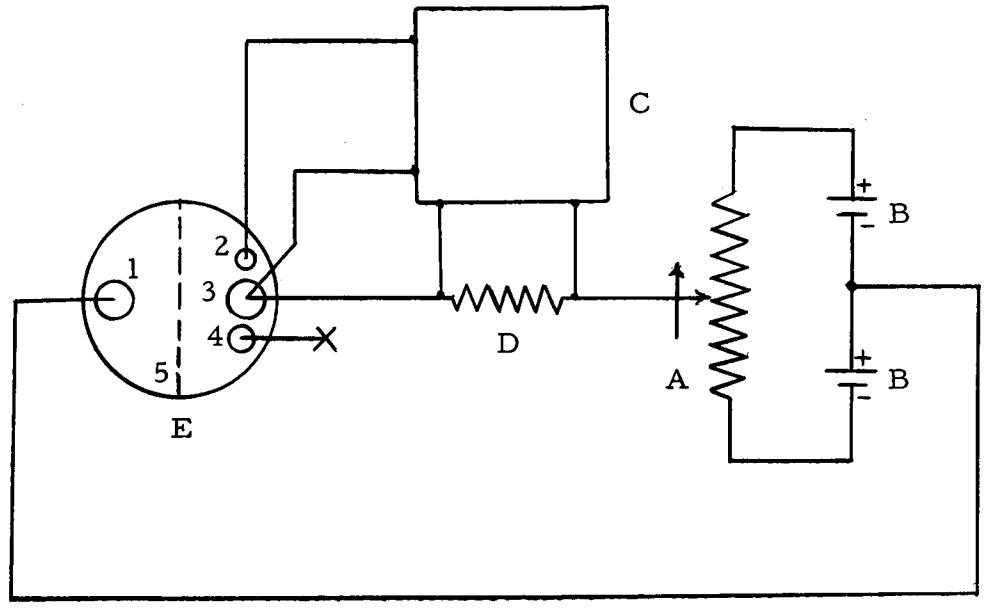

Fig. 11. Schematic diagram of electrical circuit for small forward and reverse current anode polarization measurements.

proportional to cell current. Major components shown in Fig. 11 are:

A) An 100 ohm, five watt precision potentiometer.* The potentiometer circuit was capable of a continuous variable voltage output adjustable between 1.5 to -1.5 volts.

B) Two number six, 1.5 volt dry cell batteries.

C) An x-y recorder# to simultaneously record cell current and anode reference potential. Recorder input impedance was 200,000 ohms per volt.

D) A precision shunt resistor°, variable from 0 to 900 ohms.

E) A cell assembly, which consisted of:

1) the cathode
2) the gas reference electrode
3) the graphite anode
4) the graphite reference electrode (not used)
5) a separator of gold alloy sheet to prevent large scale mixing of electrolyte in the cell.

Experimental Procedure

The anode polarization near the open circuit potentials was determined by recording the gas reference to anode potential as a

---

* Model T-10, Helipot Corporation, South Pasadena, California.

\# Model 135, F. L. Moseley Co., Pasadena, Calif.

° Cat. No. 4773, Leeds and Northrup Co., Philadelphia, Penn.

function of current passing between the working cathode and anode. The technique used to collect data was to pass a high current initially through the cell and then measure anode polarization for decreasing current settings until zero current flow was reached. Next a high reverse or charging current was passed through the cell and the anode to reference electrode potentials were again recorded for currents which decreased in magnitude to zero.

Instead of continuously recording the anode potential as a function of cell current, the anode reference potential was allowed to come to steady state after each change in the cell current before the datum point would be recorded by lowering the stylus on the paper. Currents passed through the cell were small enough so that the anode potentials reached a steady state value in about three seconds. Current-potential measurements were taken about two minutes apart, and reproducibility was within $\pm$ five millivolts for each run.

For all experiments, the cathode was supplied with an equimolal mixture of dry oxygen and carbon dioxide at about 0.20 milliliters per second. The gas reference electrode was operated as outlined in the operating procedure section of Chapter III.

Results

Anode polarization data taken for both positive and negative anode current densities (positive current is defined to be the direction

of spontaneous current flow for a cell under load) are given in Tables XI and XII. These data are also presented in Figs. 12 and 13 where the arrows indicate the directional sense of the linear extrapolation of the data.

It is evident from the curves of Figs. 12 and 13 that the same anode potentials are reached within a few millivolts for the extrapolation to zero current density from either direction. Thus it is shown that the anode reaction is kinetically reversible. That is, because no discontinuity exists in the cell potential determined by the extrapolation to zero from both positive and negative values of current densities, a smooth transition to a cathodic or to an anodic electrochemical reaction, respectively, occurs at the graphite electrode when either the anode potential is raised or lowered an infinitesimal amount above or below the open circuit potential.

Discussion of Results

Since any of several electrode reaction schemes might be responsible for the observed behavior of the graphite anode near zero current densities, several types of anode reactions will be considered and arguments for and against such reactions will be presented.

Concentration cell hypothesis

A treatment of fused carbonate indirect fuel cells by Chambers

Table XI. Anode Polarization for Low Positive and Negative Current Densities at 700°C.

Anode surface area: 17.4 cm^2

Open circuit potential: 0.68 volts

i(ma/cm^2)	E (volts)	η(volts)
5.25 (10^{-2})	0.535	0.145
4.62	0.550	0.130
4.15	0.570	0.110
3.52	0.585	0.095
2.90	0.600	0.080
2.30	0.620	0.060
1.87	0.635	0.045
1.26	0.650	0.030
0.488	0.670	0.010
*-5.08	0.750	-0.070
-4.60	0.745	-0.065
-3.99	0.737	-0.057
-2.80	0.725	-0.045
-2.27	0.720	-0.040
-1.69	0.712	-0.032
-1.09	0.700	-0.02
-0.544	0.690	-0.01

* Negative current values indicate graphite anode reaction is forced backwards to the spontaneous direction of discharge.

Table XII. Anode Polarization for Low Positive and Negative Current Densities at 860°C.

Anode surface area: 17.4 cm^2

Open circuit potential: 0.885

i(ma/cm^2)	E (volts)	η (volts)
1.31	0.840	0.045 (-0.010)
1.19	0.845	0.040
0.925	0.852	0.033
0.615	0.860	0.025
0.374	0.869	0.014
0.178	0.875	0.010
0.0575	0.882	0.003
-1.35	0.912	-0.027
-1.02	0.910	-0.025
-0.786	0.905	-0.020
-0.567	0.900	-0.015
-0.390	0.896	-0.011
-0.178	0.890	-0.005
-0.017	0.886	-0.001

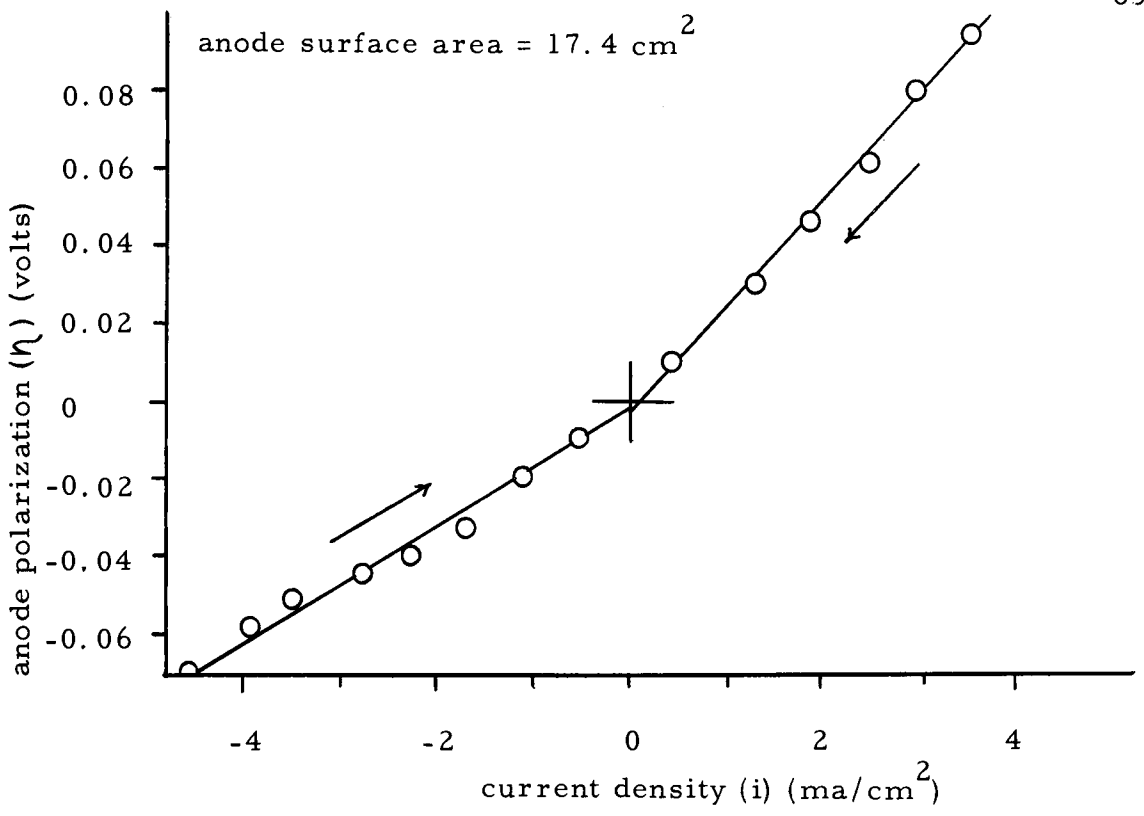

Fig. 12. Anode polarization near zero current density at 700°C.

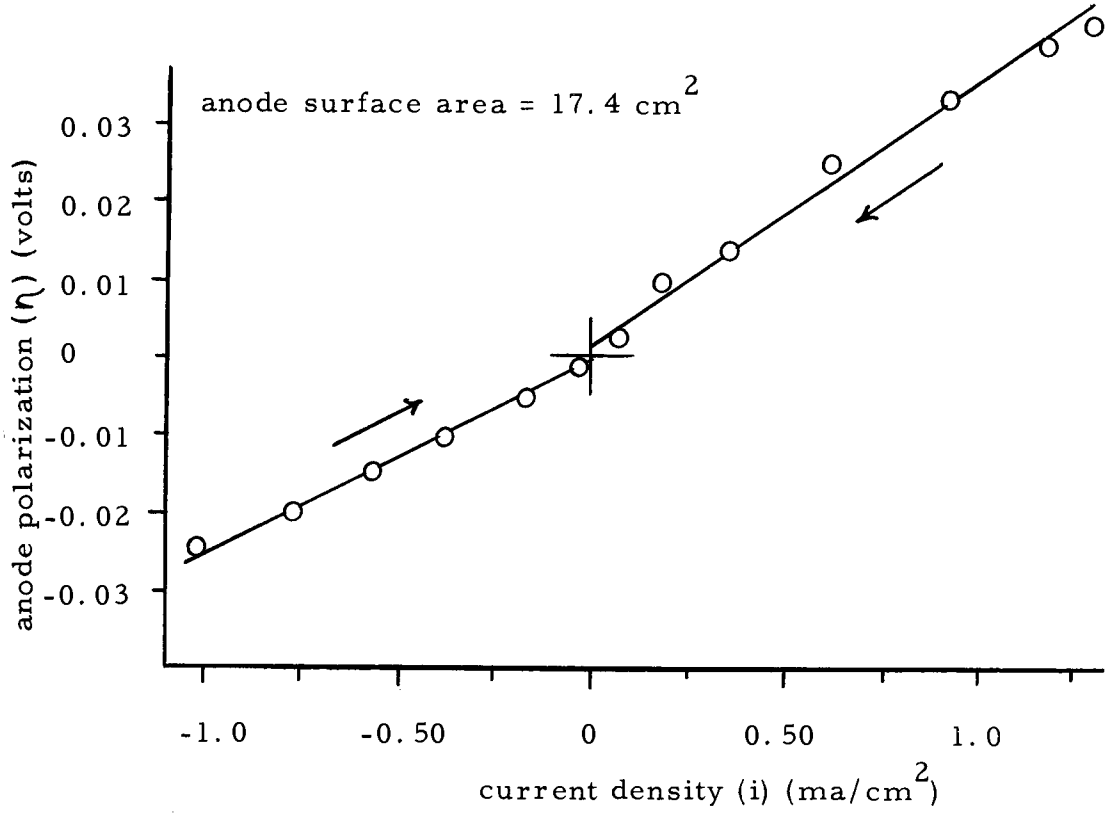

Fig. 13. Anode polarization near zero current density at 860°C.

and Tantram (9) considered the cell as an oxygen concentration cell with a fuel-depolarized anode. Strong evidence is given for this hypothesis of an oxygen concentration cell for electrodes immersed in a sodium, potassium, lithium carbonate mixture contacted by oxygen and carbon dioxide. The cathode reaction in a carbonate electrolyte cell with a mixed oxygen-carbon dioxide feed is

$$O_2 + 2CO_2 + 4e = 2CO_3^{=}. \tag{14}$$

The anode reaction at a wire contacting the electrolyte for low current densities would be

$$2CO_3^{=} = 4e + 2CO_2 + O_2. \tag{15}$$

The net cell reaction is the sum of Eq. (14) and Eq. (15) and may be written as

$$O_2(a_{O_2})_1 + 2CO_2(a_{CO_2})_1 = O_2(a_{O_2})_2 + 2CO_2(a_{CO_2})_2 \tag{16}$$

where the subscripts 1 and 2 on the activites refer to the cathode and anode respectively. The cell emf for an equilibrium process expressed by Eq. (16) may be written as:

$$E = -\frac{RT}{4F} \ln \frac{(a_{CO_2})_2^2 \, (a_{O_2})_2}{(a_{CO_2})_1^2 \, (a_{O_2})_1}. \tag{17}$$

It was found by Chambers and Tantram that cell potentials were accurately expressed by Eq. (17) under a variety of cathodic carbon

dioxide and oxygen partial pressures. It is therefore accepted that the cathode reaction occurring at the gas reference electrode in this experiment is that expressed in Eq. (14).

For practical calculations, activities for the gaseous components are defined by choosing the standard state fugacity to be one atmosphere pressure for the pure component at the temperature under consideration. Activities in Eq. (17) may therefore be approximated by the partial pressures of the individual components in atmospheres. The high temperatures and low pressures encountered in this experiment make this a reasonable assumption.

The oxygen concentration cell concept may be applied to the graphite electrode by considering the oxygen produced in the electrochemical reaction of Eq. (15) to be chemically consumed by the graphite, thus reducing the oxygen activity to some low value at the anode. It is interesting to notice that for this anode reaction mechanism it is not necessary to state what the reaction products would be as a result of the chemical oxidation of the graphite, but only that it occurs and that the concentration of oxygen at the anode is thereby reduced.

As a test of the concentration cell hypothesis, observed open circuit potentials at several temperatures, together with the estimated oxygen and carbon dioxide activities at the cathode and carbon dioxide activity at the anode, will be substituted into Eq. (17) and

oxygen activity at the anode calculated. Since the equimolar cathode gas mixture was introduced at approximately one atmosphere pressure, the activities $(a_{O_2})_1$ and $(a_{CO_2})_1$ can be set equal to 0.50. Furthermore, the activity of CO_2 at the anode may safely be assumed to lie somewhere between the decomposition pressure of fused carbonate at the temperature under consideration and unity. By reference to Eq. (4) it can be seen that by assuming the lowest possible value of $(a_{CO_2})_2$, a maximum value of $(a_{O_2})_2$ would be obtained. Therefore the actual value of $(a_{O_2})_2$ required to explain the observed emf would have to be less than or equal to this calculated value.

Experimental decomposition pressure data of Kröger and Fingas (24) for fused lithium carbonate has been fitted by Broers (8, p. 101) to the equation

$$\log P_d = - \frac{6.04\,(10^3)}{T} + 3.92 , \qquad (18)$$

where pressure P_d is in atmospheres and T in degrees K.

Similarily data of Howarth and Turner for sodium carbonate was fitted to

$$\log P_d = - \frac{8.40\,(10^3)}{T} + 3.96 . \qquad (19)$$

Broers also estimated the potassium carbonate decomposition pressure as

$$\log P_d = -\frac{10.2(10^3)}{T} + 3.93. \quad (20)$$

If an ideal mixture, and therefore a vapor pressure contribution proportional to the mole fraction of a component, may be assumed, the partial pressure of carbon dioxide from the thermal decomposition of a 4:3:3 molar ratio of fused carbonate mixture containing lithium carbonate, sodium carbonate, and potassium carbonate, respectively, is

$$\log P_{mix} = -\frac{6.07(10^3)}{T} + 4.57. \quad (21)$$

Presented in Table XIII are the observed open circuit potentials at several temperatures (see Fig. 14), calculated values of $(a_{CO_2})_2$ from Eq. (21), and calculated maximum oxygen partial pressures from Eq. (17).

Table XIII. Calculated Values of Oxygen and Carbon Dioxide Activities for Oxygen Concentration Cell.

Temperature	$E_{o.c.}$ (volts)	$(a_{CO_2})_2$	$(a_{O_2})_2$
600°C	0.55	$4.2(10^{-3})$	$1.3(10^{-8})$
700°C	0.69	$2.1(10^{-2})$	$1.3(10^{-11})$
800°C	0.82	$8.1(10^{-2})$	$1.6(10^{-14})$
900°C	0.95	$2.5(10^{-1})$	$7.9(10^{-16})$
1000°C	1.09	$4.0(10^{-1})$	$4.0(10^{-17})$

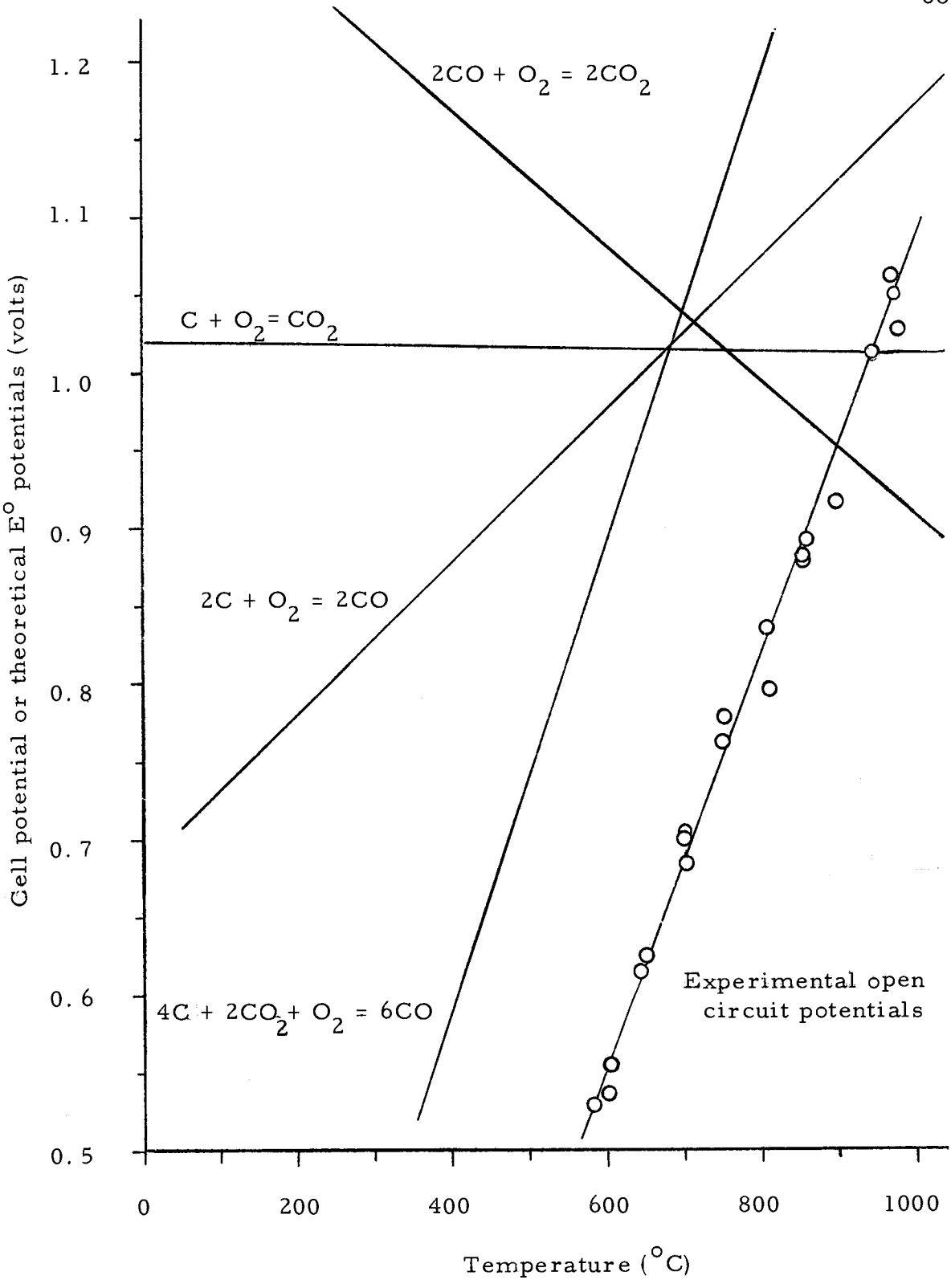

Fig. 14. Experimental cell open circuit potentials and theoretical E° values.

The calculated values of oxygen activity (numerically equal to the partial pressure in atmospheres) in Table XIII decrease rapidly with increasing temperature, which can be easily explained by the much greater chemical reactivity of graphite at higher temperatures. It should be remembered, however, that the above partial pressure values of oxygen at the anode represent a set of maximum values, and the actual oxygen pressures must be lower than the calculated values if the oxygen concentration cell model is valid.

The objection to the oxygen concentration model is based on the extremely low oxygen partial pressures required to achieve the observed cell emf. Of course such low oxygen partial pressure values are not impossible, but they seem even more improbable when one considers the chemical oxidation rates of graphite that should occur in the presence of fused carbonate electrolyte saturated with oxygen.

A rough estimate of the oxygen activity $(a_{O_2})_s$ in the saturated electrolyte was made by measuring the potential between a platinum wire, exposed only to the electrolyte, and the gas reference electrode, which had an equimolar mixture of carbon dioxide and oxygen supplied to it at about one atmosphere pressure. The electrolyte was kept saturated with respect to the oxygen and carbon dioxide by the continuous bubbling of a equimolar mixture of the gas through it. Potentials were measured for temperatures between 580°C and 980°C

and were found to be 24 $\pm$ 8 millivolts for all temperatures. Using an average value of 24 millivolts, a value of

$$(a_{O_2})_s \ (a_{CO_2})_s^2 = 0.0482 \qquad (22)$$

is obtained using Eq. (17). Making the assumption the $(a_{O_2})_s \simeq (a_{CO_2})_s$, a value of 0.36 atmospheres for the oxygen partial pressure is obtained.

If data relating the partial pressure of oxygen to the concentration of oxygen in the electrolyte were available in the literature, an estimate of the oxygen transport by diffusion to the anode, with consequent oxidation of the graphite, might be made. However, lacking such an estimate, it still seems implausible that such a low oxygen activity at the graphite surface could be maintained, yet not result in the rapid non-electrochemical oxidation of the graphite anode. That this erosion of graphite electrodes during long open circuit operation does not occur is seen in the fact that the graphite reference electrode mass loss was less than one milligram for a five square centimeter electrode operated for two weeks at temperatures varying between 600°C and 940°C.

The direct carbon monoxide cell (I)

It was shown by Baur, Peterson, and Füllemann (see Chapter II) that open circuit potentials for temperatures between 950°C to

1300°C correspond to an overall cell reaction of

$$2C + O_2 = 2CO. \qquad (3)$$

The cell was different from that used in this work in that fused borax ($Na_2B_4O_7$) instead of fused carbonate was used as the electrolyte, and copper or lead oxide cathodes were used in place of an oxygen-carbon dioxide gas electrode. Baur's oxide electrodes, in effect, were pure oxygen electrodes, where the oxygen activity was fixed by the thermal decomposition pressure of the oxide. If the oxide ion species, $O^=$, exists in the fused borax, the cathode reaction is simply

$$O_2 + 4e = 2O^=. \qquad (23)$$

The anode reaction for carbon monoxide formation is

$$2C + 2O^= = 2CO + 4e. \qquad (24)$$

The sum of reactions (23) and (24) results in the overall cell reaction of Eq. (3).

For the present system under study, however, it had been concluded in the previous discussion on concentration cells, that the carbon dioxide-oxygen cathode reaction is

$$2CO_2 + O_2 + 4e = 2CO_3^= . \qquad (14)$$

In a fused carbonate cell the $O^=$ species may be written as the carbonate ion, and the half cell reaction at the anode then becomes

$$2C + 2CO_3^= = 2CO + 2CO_2 + 4e. \qquad (25)$$

The sum of the half cell reactions (14) and (25) also give an overall carbon monoxide-oxygen cell reaction as written in Eq. (3).

Using the assumption that the emf values of the cell measured under conditions of open circuit are reversible in the thermodynamic sense, the equation expressing the cell potential is

$$E_{o.c.} = E^{o} - \frac{RT}{4F} \ln \frac{(a_{CO})_2^2 \quad (a_{CO_2})_2^2}{(a_c)_2^2 \quad (a_{CO_2})_1^2 \quad (a_{O_2})_1} \quad . \qquad (26)$$

In Eq. (26), the unknown quantities are the activities of carbon monoxide and carbon dioxide at the anode. The activity of solid pure graphite may be set equal to unity, the activities of carbon dioxide and oxygen may be approximated by the partial pressure of 0.5 atmospheres, and E^{o} values may be calculated from thermodynamic data. The partial pressure of carbon dioxide at the anode is bounded by the carbonate decomposition pressure as estimated by Eq. (21) and the vapor pressure of carbon dioxide over the saturated electrolyte. If the value of $(a_{CO_2})_2$ is set equal to $(a_{O_2})_s$ in the saturated electrolyte (calculated to be 0.36 atmospheres - see page 70), the value of $(a_{CO})_2$ calculated from Eq. (26) represents a minimum possible value.

Table XIV. Minimum Calculated Values for Carbon Monoxide Activities for the Direct Carbon Monoxide Cell(I)

Temperature (°C)	$E_{o.c.}$ (volts)	E^{o*} (volts)	$(a_{CO})_2$
600	0.55	0.975	10^5
700	0.69	1.025	$3.5(10^3)$
800	0.82	1.072	260
900	0.95	1.120	29.5
1000	1.09	1.170	4.36

* E^o values in Table XIV are calculated from thermodynamic data compiled by Wicks and Block (32).

The above calculated minimum values for the carbon monoxide activity at the anode, being numerically approximated by the partial pressure in atmospheres, are clearly impossible, and so the conclusion is reached that either the open circuit potential measurements are not thermodynamically reversible values or the assumed cell reaction is incorrect.

The direct carbon monoxide cell (II)

A modified version of the carbon monoxide cell discussed previously can be considered by writing the graphite anode reaction as

$$4C + 2CO_3^{=} \rightleftharpoons 6CO + 4e, \qquad (27)$$

instead of as in Eq. (25). Combining Eq. (27) with Eq. (14) the overall cell reaction becomes

$$4C + 2CO_2 + O_2 = 6CO. \tag{28}$$

The cell emf for reaction (28) above is

$$E_{o.c.} = E^o - \frac{RT}{4F} \ln \frac{(a_{CO})_2^6}{(a_C)_2^4 \, (a_{CO_2})_1^2 \, (a_{O_2})_1}. \tag{29}$$

Using the same assumptions made in the treatment of the carbon monoxide cell, a calculated minimum value for the carbon monoxide activity at the anode can be estimated. These values are tabulated in Table XV.

Table XV. Calculated Minimum Values for Carbon Monoxide Activities in the Direct Carbon Monoxide Cell (II)

Temperature (C°)	$E_{o.c.}$ (volts)	E^o (volts)	$(a_{CO})_2$
600	0.55	0.894	14.6
700	0.69	1.03	11.0
800	0.82	1.17	8.95
900	0.95	1.33	9.00
1000	1.09	1.48	7.55

The calculated carbon monoxide activities in Table XV are not as high as those calculated for the first type of carbon monoxide cell,

but the $(a_{CO})_2$ values are still unrealistic in that they are at least an order of magnitude too high. As a consequence, either the assumption that the cell is thermodynamically reversible must be rejected, or the cell reaction may not be represented by Eq. (28).

It is interesting to note that the experimental open circuit potentials plotted in Fig. 13 closely parallel the theoretical E^o potentials. However, only the temperature coefficient of a reversible galvanic cell may be written as

$$\left(\frac{\partial E}{\partial T}\right)_p = \frac{\Delta S}{nF}, \tag{30}$$

where ΔS is the entropy change for the reaction. Therefore Eq. (30) applies only to the calculated E^o values and not to the experimental open circuit values. In this light, the close agreement in the temperature coefficient between the assumed cell reaction in Eq. (28) and the observed open circuit potentials is believed to be more fortuitous than theoretical.

The carbon monoxide to carbon dioxide cell

Instead of attempting to explain the observed open circuit cell potentials for the various temperatures by considering only direct cells using graphite as the electrochemical reactant at the anode, a two step process may be considered to occur, whereby carbon monoxide serves as the reactive electrochemical constituent. It is proposed that the first step in the anode reaction is the

thermochemical Boudard shift, where carbon dioxide combines with graphite to form carbon monoxide; the second step is the electrochemical oxidation of carbon monoxide to carbon dioxide. The two reaction steps at the anode are

$$C + CO_2 = 2CO, \tag{31}$$

and

$$2CO + 2CO_3^{=} = 4CO_2 + 4e, \tag{32}$$

and the overall anode reaction becomes

$$C + 2CO_3^{=} = 3CO_2 + 4e. \tag{33}$$

Combining Eq. (33) with the cathode reaction (14), it is seen that the overall cell reaction corresponds to the direct oxidation of carbon to carbon dioxide:

$$C + O_2 = CO_2. \tag{4}$$

However, an interesting point to be noticed in the two step mechanism above is that the cell potential is not determined by Eq. (4), but only by the electrochemical processes represented by the sum of Eq. (32) and Eq. (14), i.e.,

$$2CO + O_2 = 2CO_2. \tag{34}$$

The theoretical cell potential for Eq. (34) is

$$E_{o.c.} = E^{o} - \frac{RT}{4F} \ln \frac{(a_{CO_2})_2^{4}}{(a_{CO})_2^{2} (a_{CO_2})_1^{2} (a_{O_2})_1}. \tag{35}$$

For the equilibrium process, the activities $(a_{CO})_2$ and $(a_{CO_2})_2$ are related by the standard free energy change of the Boudard reaction in the following manner:

$$\Delta F^{o}_{(31)} = -RT \ln \frac{(a_{CO_2})_2^2}{(a_{CO})_2 (a_C)_2} , \qquad (36)$$

where the subscript (31) of ΔF^{o} refers to the standard free energy change of the reaction in Eq. (31). Solving for $(a_{CO})_2^2$ and substituting into Eq. (35), we obtain

$$E_{o.c.} = E^{o}_{(34)} - \frac{RT}{4F} \ln \frac{(a_{CO_2})_2^2}{(a_{CO_2})_1^2 (a_{O_2})_1 (a_C)_2} - \frac{\Delta F^{o}_{(31)}}{4F} . \qquad (37)$$

Substituting values of the observed cell potentials and thermodynamic data as described previously into Eq. (37), numerical values of $(a_{CO_2})_2$ are calculated and tabulated in Table XVI.

From Table XVI it is seen that low temperature values of $(a_{CO_2})_2$ are much too high, while for high temperature operation values of $(a_{CO_2})_2$ approach the decomposition pressures of the fused electrolyte. A similar conclusion is made, as before, that either the cell is thermodynamically irreversible or the cell reaction does not

occur by the proposed two step process.

Table XVI. Calculated Minimum Values for Carbon Dioxide Activities in the Carbon Monoxide to Carbon Dioxide Cell

Temperature (°C)	$E_{o.c.}$ (volts)	$E^{o}_{(34)}$ (volts)	$\Delta F^{o}_{(31)}$ (cal/mol)	$(a_{CO_2})_2$
600	0.55	1.082	-4,040	6,400
700	0.69	1.040	-1,170	144
800	0.82	0.916	-5,440	7.62
900	0.95	0.952	-9,660	0.588
1000	1.04	0.910	-10,380	0.060

The direct carbon cell

According to experimental work on the carbon oxygen fuel cell performed by Tamaru and Kamada (31), the low temperature electrochemical cell reaction corresponds to:

$$C + O_2 = CO_2, \tag{4}$$

The corresponding half cell reactions are, at the cathode:

$$2CO_2 + O_2 + 4e = 2CO_3^{=}, \tag{14}$$

and at the anode:

$$C + 2CO_3^{=} = 3CO_2 + 4e . \tag{33}$$

The theoretical cell potential is expressed as

$$E_{o.c.} = E^{o} - \frac{RT}{4F} \ln \frac{(a_{CO_2})_2^3}{(a_{CO_2})_1^2 \, (a_{O_2})_1 \, (a_C)_2} . \quad (38)$$

As in the treatment of the carbon monoxide cell, substitution of estimated values for $(a_{CO_2})_1$, $(a_{O_2})_1$, and $(a_C)_2$ and values of E^o, calculated from thermodynamic data, into Eq. (38), one can calculate the activity of carbon dioxide that must exist at the anode for the open circuit potential data to be explained by the reaction given by Eq. (4).

The values of (a_{CO_2}) listed in Table XVII are also clearly impossible for the 600°C to 800°C temperature range. Therefore, we are forced to admit that since Eq. (26) cannot be used to adequately explain the open circuit potential data, the cell must be operating in a distinctly irreversible manner as far as thermodynamics is concerned. This conclusion must be especially valid near 600°C, since in this area, the assumed cell reaction of Eq. (4) is known to occur.

Table XVII. Calculated Values of Carbon Dioxide Activity for the Direct Carbon to Carbon Dioxide Oxidation Cell.

Temperature (°C)	$E_{o.c.}$ (volts)	E^o (volts)	$(a_{CO_2})_2$
600	0.55	1.017	2,100
700	0.69	1.015	105
800	0.82	1.014	7.62
900	0.95	1.013	1.14
1000	1.09	1.012	0.204

Summary

The foregoing discussions have treated several models of the carbon-oxygen cell in an attempt to interpret observed cell potentials in the light of conventional reversible thermodynamics. In each case it was shown that unlikely and/or impossible numerical values for either the reactant or the product activities were necessary to explain the data, for at least part of the temperature range considered, if the cell were functioning in a truly reversible manner.

Since the observed open circuit potentials can not be thermodynamically reversible values, it is concluded that a large free energy loss must occur during the anode potential determining reaction. This large free energy loss would be reflected in open circuit potentials which are considerably lower than the true reversible value and this is believed to be due to the extreme difficulty of ionizing the carbon atoms in the surface of the graphite electrode.

Of the several models considered, only the overall cell reaction

$$C + O_2 = CO_2 \qquad (4)$$

could be explained theoretically and then the calculated values $(a_{CO_2})_2$ are reasonable only for the high temperatures of 900°C to 1000°C. It was shown that the overall cell reactions of Eq. (4) could be achieved by either a direct one step oxidation of the carbon or by a

two step process employing the Boudard shift, followed by an electrochemical oxidation of the carbon monoxide. There is special merit in the latter mechanism, but further discussion will be postponed until Chapter V.

The observed behavior of the kinetic reversibility of the anode reaction, described in the results section of this chapter and illustrated in Figs. 12 and 13, is believed to be due to a separate reaction occurring at the anode, dependent only upon the direction of the current flow. For example, for spontaneous discharge of the cell (positive current flow), the anode reaction could be

$$C + 2CO_3^{=} = 3CO_2 + 4e, \qquad (33)$$

and would continue to react according to Eq. (33) until the limit $i \rightarrow 0$ is reached. For negative currents, the reaction at the graphite electrode could be a simple decomposition of the electrolyte such as

$$2e + 2M_2CO_3 = 2M_2O + CO + CO_3^{=} \qquad (39)$$

or

$$4e + 3M_2CO_3 = 3M_2O + C + 2CO_3^{=}, \qquad (40)$$

where M represents an alkali metal as sodium, potassium, or lithium.

It is not understood exactly what does happen at the graphite electrode for negative currents, but it seems certain that the reverse

reaction of Eq. (33) does not occur, and therefore the anode reaction is distinctly irreversible during open circuit operation.

V. EXPERIMENTS ON ANODE REACTION PRODUCTS

The Need for the Study

A series of experiments to determine the products of the anode reaction for several current densities and temperatures were undertaken for the following reasons: First, it was desirable to determine if any major change in the anode reaction occurs under current drain between a low temperature of 600°C where Tamaru and Kamada (31) showed the overall cell reaction is

$$C + O_2 = CO_2 , \tag{4}$$

(see previous work in Chapter II) and the high temperatures of 950°C where Baur and co-workers (3) concluded the cell reaction, according to thermodynamic considerations, is

$$2C + O_2 = 2CO . \tag{3}$$

Of additional interest would be knowledge of the anode gassing rates for various cell currents and temperatures, which could lead to certain conclusions with respect to possible overall anode reactions.

Techniques and Design Factors

Analysis of the gaseous anode reaction products was carried out by vapor chromatography. The gas collected in the anode compartment was conducted through a very small bore stainless steel tubing to the chromatograph sampling valve, through the

chromatograph sampling system, through a calcium chloride drier, then into a 50 milliliter buret. The progress of the gas down the buret tube was marked by a soap bubble film adhering to the interior walls of the tube. The soap bubble, marking the volume displacement, was free to move almost frictionlessly along the wetted interior. The position of the bubble could be measured very accurately using the markings on the buret. Timing the soap film between marks with a stop watch permitted the calculation of the anode gassing rate to within two percent accuracy. The calcium chloride drying tube was installed in the sample line between the buret and the sample valve to prevent accidental diffusion of water vapor from the buret metering system back through the sample valve and into the cell. Soap bubbles were injected into the buret cylinder by squeezing a rubber bulb filled with soap solution that was mounted on the gas inlet end of the buret. Gas flowing through the system then blew the liquid into a bubble, thus sealing off the cross section of the buret, whereupon the film then moved along the tube at the gas flow rate.

Use of the vapor chromatograph provided a quick accurate method of gas analysis using only a one milliliter sample of the gas. This feature of small sample volume requirements was also desirable from the standpoint of minimum gas collection and cell reaction times. As mentioned in Chapter III on the polarization experiments, the use of a simple metal cathode results in the decomposition of the

electrolyte when current is forced to flow through the cell, even at moderately low current densities. Preliminary experiments showed the driven cathode reaction resulted in large quantities of carbon monoxide being evolved and the deposition of carbon on the cathode. It is speculated both reactions result in the formation of alkali oxides as follows:

carbon monoxide formation,

$$2e + 2M_2CO_3 = 2M_2O + CO + CO_3^{=} , \qquad (39)$$

carbon formation,

$$4e + 3M_2CO_3 = 3M_2O + C + 2CO_3^{=} ,$$

where M represents the alkali metals, sodium, lithium, or potassium. Clearly, it would be desirable to keep to a minimum the formation of the alkali oxides in order to prevent possible side effects at the anode due to the build up of such compounds during cell discharge. Possible side effects due to this oxide formation are minimized in this experiment not only by keeping the cell discharge time as short as possible, but by limiting electrolyte bulk motion between the anode and cathode compartments. A gold alloy sheet diaphragm attached to the sides of the crucible and dividing the crucible into two parts was used to minimize such intermixing. The diaphragm was held in place with tabs bent over the sides of the crucible thus allowing enough clearance around the edges to permit adequate

electrolytic conductance between the compartments. To remove the alkali oxide formed during the cell discharge, pure dry carbon dioxide was continuously bubbled into the melt through the gold alloy tube which also served as the cathode. The reaction consuming M_2O was:

$$CO_2 + M_2O = M_2CO_3 . \quad (41)$$

In order to collect the gases evolved from the anode without direct intermixing with the gas environment inside the furnace, a bell mouth gas collector of gold alloy was mounted above the active section of the graphite anode. The bottom of the collector was submerged one and one half centimeters beneath the electrolyte surface. Gas collected in the bell mouth displaced the electrolyte, and the hydrostatic pressure then forced the accumulating gas out through the chromatograph sampling system into the gas volume measuring apparatus as rapidly as it was formed. Care was taken to insure that the metal collector was electrically insulated from the anode to prevent short circuiting of the graphite anode, thus resulting in the anodic dissolution of the gold alloy collector.

Of particular importance to the successful operation of the bell mouth collector is the requirement that adequate annular cross-sectional area be available for unrestricted passing of the gas bubbles through it. It is also essential that space be left inside the collector above the electrolyte for efficient separation of the electrolyte from

the gas bubbles arriving at the liquid surface. Failure to do so results in entrained electrolyte forming bubbles at the mouth of the outlet tube which are forced up through the tube until they reach the cooler upper section of the tube where the carbonate salt freezes solid completely blocking the tube. To aid in the prevention of plugging, it was found necessary to resort to a 3.95 millimeter inside diameter outlet tube which was large enough to further separate the liquid from the rising gas in the tube if it did gain entrance to it.

The above mentioned design requirements for successful gas collection and liquid separation preclude a gas collection system having a small volume. This small volume is desirable from the standpoint of obtaining a representative sample of gas with a minimum dilution or mixing with gases already present in the system. In order to side step this problem of undue sample dilution by gases from a previous run, the entire sampling system was purged between gas analysis runs with helium gas. Since the purging gas was identical to the carrier gas in the chromatography apparatus, only the components other than helium which were generated in the anode compartment would be detected in the thermal conductivity analyzer unit of the chromatograph. This helium purge method offered the very decided advantage of not having to waste a large part of the anode reaction gas, which otherwise would have to be generated to purge the system adequately.

The calculated volume of the sampling system was 3.7 milliliters. When a one milliliter sample was taken after three milliliters of anode gas had been generated, the analysis indicated a higher concentration in carbon monoxide than did a run where four milliliters of gas had been generated under the same conditions of temperature and current density. This was to be expected since the diffusivity of carbon monoxide in helium is about 22 percent higher than that of carbon dioxide in helium. Runs where five milliliters of gas were evolved before a sample was taken for analysis duplicated the results of the four milliliter run.

An additional problem in the analysis arose because of very rapid back diffusion of helium through the anode gas inside the sample collector and gas outlet tube causing the actual concentration of the helium in the sample tube to be as high as 90 percent at the end of the sampling period. The remaining ten percent of the gas sample therefore consisted of the gases of interest, which must be separated in the chromatograph for the analysis. Such low concentrations make the sample very sensitive to such impurities as air gaining entrance through very small leaks, although extreme caution was taken to prevent the existence of leaks in either the gas collection system or the gas outlet tube and external connections of the sampling system. Any air present in the sample was observed as the first peak on the chromatogram.

To reduce the concentration of air in the furnace during cell operation, a helium inlet was installed in the top of the furnace, and, although up to three liters per minute of helium were fed into the furnace, it was possible for air to enter the furnace from the bottom of the furnace tube and diffuse up through the annular space between the outer furnace tube and the adjustable crucible support tube. Attempts were made to seal off this source of air by packing asbestos paper around the bottom of the furnace tube. Analysis of the furnace atmosphere from time to time during the experiment revealed the concentration of air varied from 1.3 percent to six percent by volume for a helium purging rate of one liter per minute. The free volume inside the furnace was about 0.6 liters.

Further comment should also be made about the design for the anode-gas collector diagrammed in Fig. (16). The method of supporting the anode is very similar to that used in the polarization studies of Ch. III since the platinum wire was pushed into a drilled hole in the graphite to support the electrode. The long neck of the graphite anode was to protect the platinum wire from the anodic attack that would occur if it were exposed directly to the electrolyte during high current density runs. The anode mounting wire was supported in the center of the large I. D. alumina tube by three small platinum wires fused at right angles to the mount wire. These small wires were slightly longer than the inside diameter of the outlet tube

and were fastened to the center wire 120° apart and three millimeters above the other. Installation of the anode and mounting wire into the outlet tube was done by merely drawing the mounting platinum wire up into the tube, whereupon the cross wires bent down slightly. This tightly wedged the central wire into position yet allowed adequate free cross-sectional area for gas flow. The gold alloy bell mouth and collector shell were mounted on the outside of the alumina gas outlet tube and sealed by injecting cement between the gold sleeve and outlet tube, and then filleting cement around the joints.

Equipment

The cell and gas collection system required for this study are shown in Fig. 15. The apparatus depicted consisted of the following parts:

1) A gas chromatograph* using a separation column of crushed silica gel of 35-65 mesh contained in a 1/4 inch glass tube, 74 inches long. The chromatograph had a thermal conductivity detector element which was capable of measuring a component whose concentration was as small as 0.05 percent under the conditions of the experiment.

* A Perkin-Elmer Model 154, Norwalk, Connecticut.

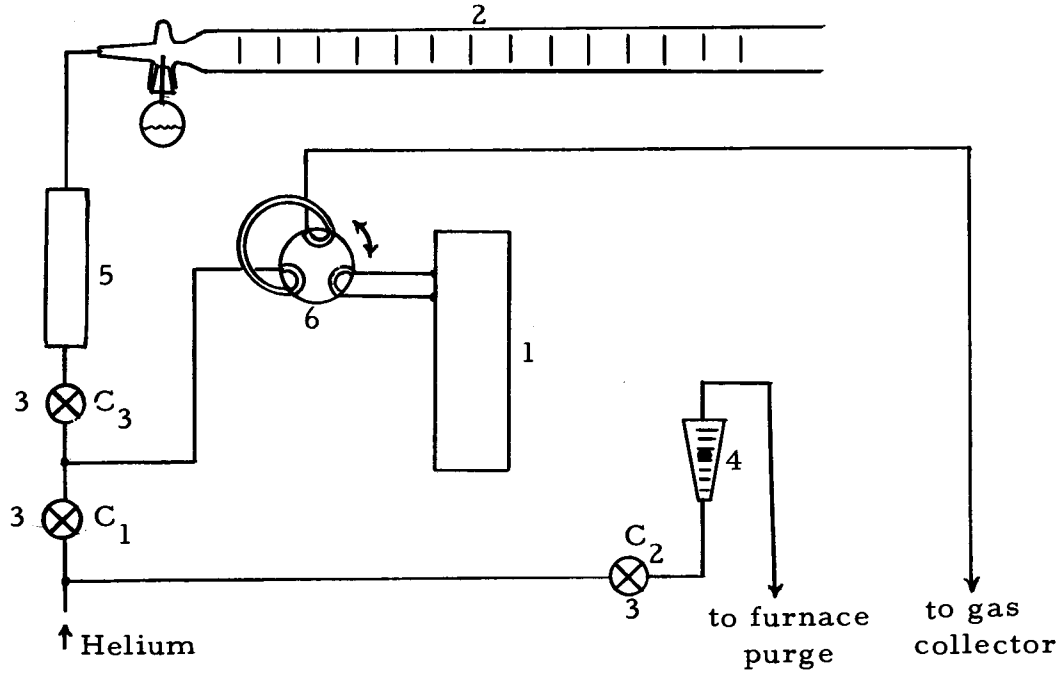

Fig. 15. Schematic diagram of gas analysis system.

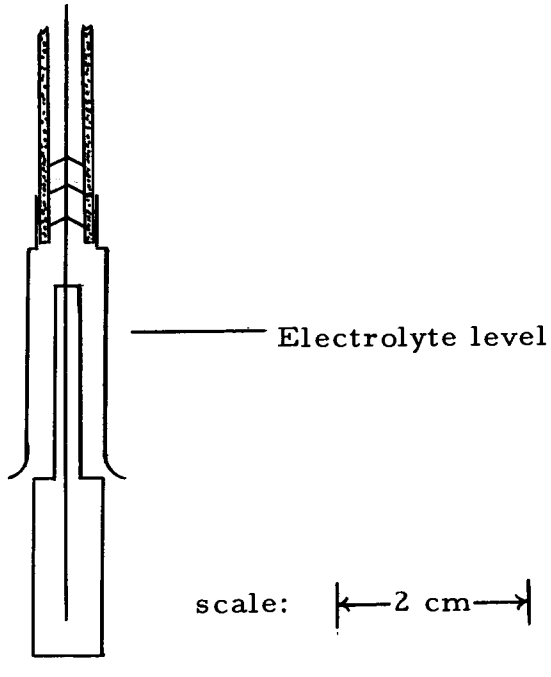

Fig. 16. Drawing (to scale) of the gas collector and anode support assembly.

2) A regular 50 ml buret with stopcock removed and rubber bulb soap injector fitted into the tapered fitting. Injecting soap into the inlet of the buret while gas was flowing through formed soap films stretched across the buret cross-section. This soap film marked the flow of gas through the buret tube.

3) Needle valves for control of helium gas. The gas used was from the same helium bottle used to supply the chromatograph carrier gas.[#] The helium was regulated at 20 psi with the pressure regulator mounted on the high pressure storage bottle.

4) A flow meter[o] of three and one half liters per minute maximum capacity to meter the helium flow.

5) A calcium chloride drying tube to prevent possible back diffusion of water vapor from the soap solution in the buret into the chromatograph sampling tube and into the cell.

6) A six port sample valve fitted with a one milliliter sample tube.

[#] National Cylinder Gas Co., Eugene, Oregon.

[o] No. 01-150/13, Fisher Scientific Co., Portland, Oregon.

Experimental Procedure

About 116 grams of alkali carbonate eutectic mixture was fused in the cell crucible at an elevated temperature, and the electrode assembly was inserted in much the same manner as was described in the procedure for the anode polarization experiments. Care was taken to insure proper anode and gas collector positioning in the electrolyte. Proper electrode depth of 1.5 centimeters as indicated in Fig. 15 was attained by adjusting the crucible height in the furnace. The helium furnace purge gas was turned on and set at one liter per minute at least 15 minutes before each experiment. The gas collector, outlet tube and sample valve assembly were also purged with helium at a flow rate of approximately six ml/min. This helium was fed to the anode compartment at all times except when a sample was being taken, at which time the valve c_1 in Fig. 15 was closed and valve c_3 was opened to allow the anode gas to flow into the soap film buret to measure the off gassing rate and amount. The initial position of a soap film in the buret was noted and a stop watch was started when the cell current switch was turned on. Cell current was maintained essentially constant by the same external current source described in Part II. The cell current and stop watch were stopped when five milliliters of gas had been generated, after which the gas inside the one milliliter sample tube was diverted

into the chromatograph for analysis by turning the sample valve. Immediately after the sample was taken, the helium was turned on at valve c_1, and valve c_3 was closed.

The chromatograph or vapor refractometer had been previously calibrated for the following settings that were used throughout the experiment:

carrier gas pressure - 2.5 psi

carrier gas flow rate - 3.8 ml/min

oven temperature - 27°C

Under these conditions, oxygen and nitrogen were eluted in 1.00 minutes, carbon monoxide in 1.32 minutes, and carbon dioxide in 24 minutes.

Results and Conclusions

A study of the products from the anode reaction tabulated in Tables XVIII through XXI and illustrated in Fig. 17 shows that both carbon dioxide and carbon monoxide are generated at low temperatures. At high temperatures the carbon monoxide concentration becomes considerable, especially at low current densities. The relatively high concentration of carbon monoxide at high temperatures and low current densities is not too surprising in light of the increased Boudard shift, which occurs for the higher temperatures when carbon dioxide is in contact with carbon. The high carbon

Table XVIII. Analysis of Graphite Anode Reaction Products at 650°C

CO_2: 0.164 ml/sec

Anode area: 3.83 cm

Sample ml	Time min	Rate ml/min	CO %	CO_2 %	Air %	CO/CO_2 $\frac{\text{mole}}{\text{mole}} \times 10^3$	Current Density ma/cm^2
4.0	6.30	0.682	no trace of CO		-	-	23.5
4.3	2.77	1.55	0.11	94.2	5.66	1.17	35.3
4.0	2.37	1.82	0.13	95.4	4.50	1.36	44.6
5.0	2.62	1.91	0.13	96.9	2.99	1.36	70.5
4.0	2.0	2.0	0.18	97	2.83	1.77	141

Table XIX. Analysis of Graphite Anode Reaction Products at 700°C.

CO_2: 0.145 ml/sec
Anode area: 3.83 cm^2

Sample ml	Time min	Rate ml/min	CO %	CO_2 %	Air %	$\frac{CO/CO_2}{mole} \times 10^3$	Current Density ma/cm^2
5.0	3.88	1.29	0.35	43.5	56.2	8.11	18.6
5.0	2.35	2.13	0.37	67.3	32.3	5.22	35.9
4.0	1.21	3.31	0.50	76.4	23.1	6.5	47.8
4.0	1.08	3.21	0.53	84.2	15.3	6.30	69.7
5.0	1.25	4.00	0.39	84.5	15.1	4.65	77.7
5.0	1.43	3.50	0.67	86.2	13.1	7.78	77.7
4.0	0.87	4.60	0.39	78.0	21.6	5.00	106
5.0	1.03	4.86	0.67	85.4	13.9	7.86	115

Table XX. Analysis of Graphite Anode Reation Products at 800°C.

CO_2: 0.145 ml/sec

Area: 3.83 cm^2

Sample ml	Time min	Rate ml/min	CO %	CO_2 %	Air %	CO/CO_2 $\frac{mole}{mole} \times 10^2$	Current Density ma/cm^2
5.0	3.97	1.26	1.21	31.3	67.5	3.86	17.7
5.0	2.67	1.87	2.64	67.4	30.0	3.92	27.9
5.0	1.72	2.91	2.59	59.2	38.2	4.38	41.0
5.0	1.43	3.49	1.63	71.6	26.8	2.27	49.7
5.0	1.32	3.79	1.84	77.4	20.8	2.38	69.7
5.0	1.28	3.90	1.56	80.3	18.1	1.94	79.6
5.0	1.08	4.62	1.73	85.0	13.3	2.04	99.5
5.0	0.984	5.09	1.83	84.0	14.2	2.18	109.0
5.0	0.917	5.56	2.30	84.6	13.1	2.71	119.0

Table XXI. Analysis of Graphite Anode Reaction Products at 870°C.

CO_2: 0.145 ml/sec
Anode area: 3.83 cm^2

Sample ml	Time min	Rate ml/min	CO %	CO_2 %	Air %	CO/CO_2 $\frac{mole}{mole} \times 10$	Current Density ma/cm^2
5.0	1.52	3.29	10.8	16.9	72.3	6.40	14.2
5.0	3.45	1.45	11.7	22.9	65.4	5.12	17.3
5.0	1.85	2.70	12.7	46.1	41.2	2.75	28.7
5.0	1.45	3.44	12.8	60.1	27.1	2.13	41.3
5.0	1.79	2.79	11.3	67.5	21.2	1.68	53.7
5.0	0.884	5.65	9.44	75.4	15.2	1.26	80.6
5.0	0.934	5.35	9.67	78.3	12.0	1.24	89.5
5.0	0.750	6.67	10.9	78.0	11.1	1.40	107

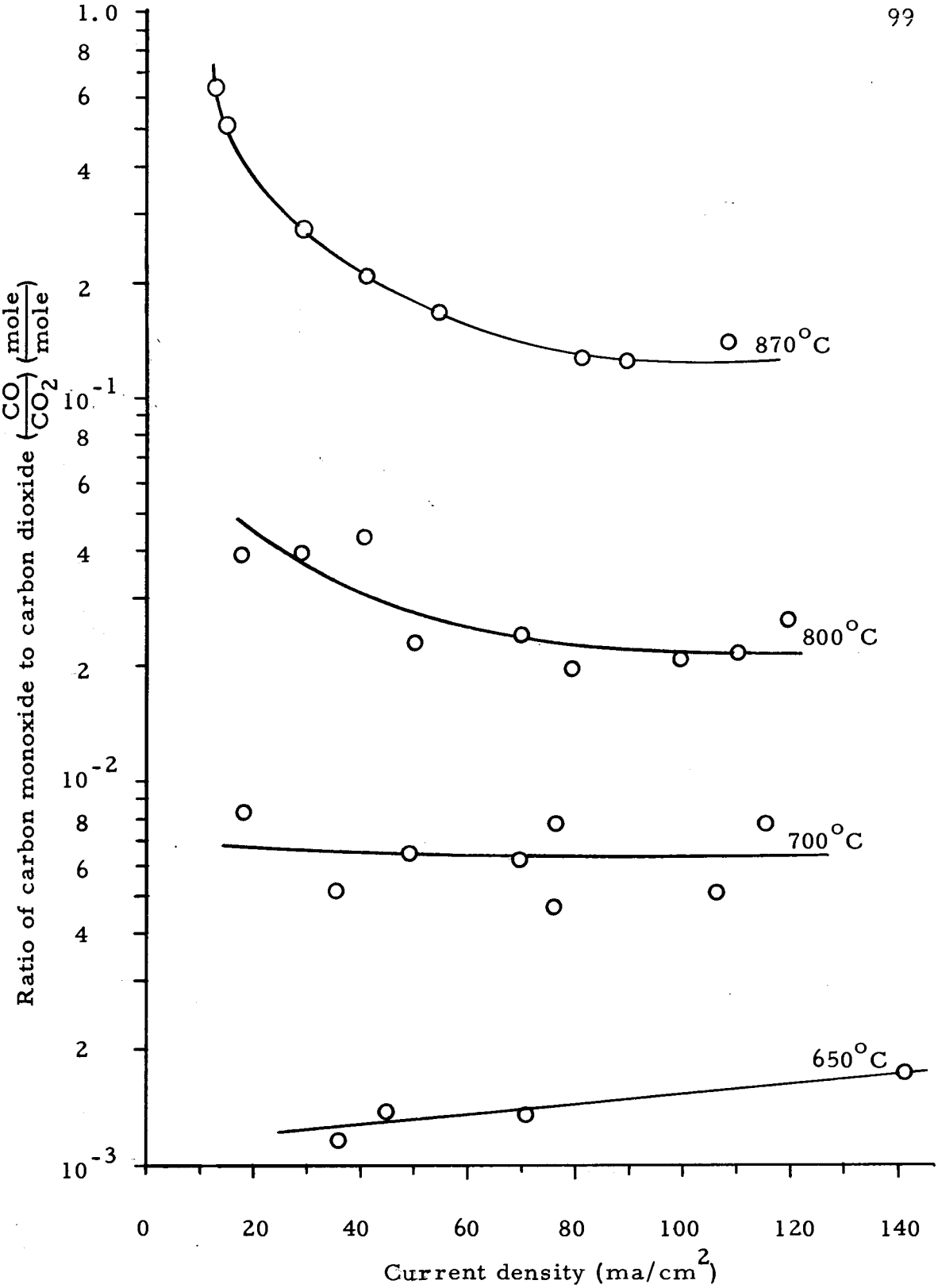

Fig. 17. Graphite anode reaction products.

dioxide concentration occurring for the higher current densities indicates the main overall cell reaction is

$$C + O_2 = CO_2 . \tag{4}$$

It is evident that the carbon dioxide present in the gaseous reaction products is produced electrochemically when one calculates the theoretical rate of carbon dioxide formation for the overall anode reaction of

$$C + 2CO_3^{=} = 3CO_2 + 4e . \tag{33}$$

It should be noted that Eq. (33) represents both the anode reaction for the direct one step oxidation model and the proposed two step model employing the two reactions

$$C + CO_2 = 2CO , \tag{31}$$

and

$$2CO + 2CO_3^{=} = 4CO_2 + 4e , \tag{32}$$

since the sum of the reactions in Eq. (31) and (32) is identical to Eq. (33).

Assuming ideal behavior for the anode gas, the theoretical rate of gas production, r, in ml/min, at the anode is

$$r = \frac{RTiA\,(10^{-3})}{nFP} \tag{42}$$

where R is the gas constant, A is the anode surface area, and P is the absolute gas pressure. The other symbols have their usual meanings.

For the overall anode reaction of Eq. (33) $n = 4/3$ and the rate of gas generation becomes, upon substitution of constants,

$$r = 11.42\,(10^{-3})\ iA, \tag{43}$$

when T is taken to be $298^{o}K$.

As a comparison to the theoretical rate, the measured carbon dioxide evolution rate is calculated by multiplying the observed gas generation rate by the fraction of carbon dioxide measured in the gas sample. Both the theoretical rates (r_{theo}) and the observed rates (r_{obs}) of carbon dioxide generation are given in Tables XXII through XXV.

A comparison of the theoretical gas generation rates based upon the measured cell current and anode half cell reaction (4) with the actual rate of carbon dioxide production shows good agreement for most of the lower current densities. It is interesting to observe that in no case does the measured carbon dioxide flow rate exceed the theoretical rate of production. At some of the high current densities a considerable discrepancy between the theoretical and actual gas evolution rates occurs, which is attributed to collector spillage because of inefficient collection of the rising gas bubbles in the electrolyte at high evolution rates.

An unresolved problem in this experiment is evident from the data which show that a rather high concentration of air is found in the anode gases. As mentioned, considerable effort was taken to ensure

Table XXII. Anode Reaction Products Gas Generation Rates at 650°C.

Anode area: 3.93 cm^2		
$r_{theo.}$ (ml/min)	$r_{obs.}$ (ml/min)	i(ma/cm^2)
1.54	1.46	35.3
1.95	1.74	44.6
3.09	1.85	70.5
6.17	1.94	141

Table XXIII. Anode Reaction Products Gas Generation Rates at 700°C.

Anode area: 4.52 cm^2		
$r_{theo.}$ (ml/min)	$r_{obs.}$ (ml/min)	i (ma/cm^2)
0.960	0.562	18.6
1.85	1.43	35.9
2.57	2.53	47.8
3.60	2.77	69.7
4.02	3.38	77.7
4.02	3.01	77.7
5.46	3.59	106
5.95	4.15	115

Table XXIV. Anode Reaction Products Gas Generation Rates at 800°C.

Anode area: 4.52 cm^2		
$r_{theo.}$ (ml/min)	$r_{obs.}$ (ml/min)	i (ma/cm^2)
0.902	0.394	17.7
1.44	1.26	27.9
1.75	1.72	33.8
4.11	3.13	39.6
2.57	2.50	49.7
3.33	2.92	69.7
4.47	3.92	99.5
5.65	4.27	109
6.38	4.72	119

Table XXV. Anode Reaction Products Gas Generation Rates at 870°C.

Anode area: 4.52 cm^2		
$r_{theo.}$ (ml/min)	$r_{obs.}$ (ml/min)	i (ma/cm^2)
0.732	0.556	14.2
0.892	0.332	17.3
1.65	1.25	28.7
2.37	2.09	41.3
3.09	1.89	53.7
4.54	4.20	80.6
5.14	4.19	89.5
6.16	5.20	107

that no gas leaks existed in either the gas outlet tube or external plumbing to the chromatograph cell. A good test for the location of a leak was to pressurize the system with helium, then apply a soap solution to all fittings and connections in the system. When the gas leaks in the system were eliminated it was possible to allow helium to remain static in the system at one atmosphere pressure for periods of up to a half hour, after which a gas sample would be switched into the chromatograph and analyzed for air content. There would be less than 0.08 percent air found in the gas tight system.

Since considerable concentration of air was found in the gas sample only after several milliliters of gas had been generated by the anode reaction, it was believed that either air was dissolving in the cell from the furnace atmosphere and was being swept out of the electrolyte by the rising bubbles from the anode, and/or air was diffusing into the system through the thin walled recrystallized alumina gas outlet tube. In order to reduce these effects, helium was used to purge the furnace atmosphere of air. After this air concentrations as low as 1.3 percent to six percent could be maintained. At first glance this would seem to severely limit the possible percentage of air in the sample. As has been pointed out, however, the gas produced by the anode reaction is diluted by the rather large volume of helium in the collection system, and at low

current densities, the helium concentration at the sample valve is as high as 90 to 94 percent. Therefore, although an air concentration as high as 67.5 percent is reported, the actual concentration in the gas stream is only about four percent.

It is of interest to note that in the work of Tamaru (31), analysis of the anode gas for the reaction occurring at 600°C showed it to contain 8.1 percent nitrogen. No indication of the method used to collect the anode gas or to analyze it was given, but it seems probable that the nitrogen originated from air dissolved in the electrolyte.

Even though it was undesirable to have the persistant appearance of air in the anode gas sample, it is believed its influence upon the concentration ratio of carbon monoxide to carbon dioxide was negligible. Of course the possibility existed for the chemical combustion of carbon monoxide to carbon dioxide, but analysis of air in the furnace atmosphere and in the anode gas sample showed the oxygen to nitrogen ratio to be essentially the same. A ten foot long by one quarter inch diameter column of 35-63 mesh activated charcoal was constructed and installed in the chromatograph to separate oxygen and nitrogen for the air determination since silica gel was incapable of this separation.

In addition to the constancy of the ratio of oxygen to nitrogen in the anode gas sample and in the furnace, more evidence that little if

any carbon monoxide was chemically oxidized to carbon dioxide is found in the carbon monoxide to carbon dioxide data plotted in Fig. 17. There, it is seen that for the highest temperature (870°C) data, the carbon monoxide to carbon dioxide ratio is highest for the lowest current density runs, which also happen to correspond to the runs where the air concentration is highest and residence times in the high temperature regions the longest. If chemical combustion occurred, this observed behavior would be highly unlikely.

In conclusion, the analysis of the gaseous anode reaction products confirm the findings of Tamura and Kamada (31) in that the main overall anode reaction is the oxidation of carbon to carbon dioxide. However, at higher temperatures, a different anode reaction becomes apparent since at low current densities up to 37 percent of the anode gas is carbon monoxide, which then decreases to nine percent for the higher current densities. The explanation for this behavior is believed to be that the reaction occurs in two steps, namely the Boudard shift followed by the electrochemical oxidation of the thermochemically produced carbon monoxide. Of course, other two or more step processes might be proposed, but if they utilize steps involving the electrochemical production of carbon monoxide, which is further reacted electrochemically in subsequent steps to carbon dioxide, the overall effect is still the direct one step oxidation of

carbon to carbon dioxide and the question becomes one of reaction mechanisms, which cannot be verified in this work.

VI. CONCLUSIONS

1) The main overall anode reaction is the complete oxidation of carbon to carbon dioxide. Moderate quantities of carbon monoxide detected during high temperature, low current density operation indicate the anode reaction is not a simple one step oxidation of carbon to carbon dioxide, but that the true reaction mechanism incorporates a step involving the formation of carbon monoxide with a subsequent electrochemical oxidation to carbon dioxide.

2) The open circuit potentials measured in the temperature range of 550°C to 900°C are much lower than the theoretically predicted values and can only be explained by a highly irreversible electrode process occurring at the anode.

3) The anode polarization data, represented in a Tafel plot, is linear for temperatures below 700°C. The slope of the Tafel plot indicates that the number of electrons transferred per reacted carbonate ion is two. A slight increase in slope, which occurs near current densities of eight ma/cm^2 for temperatures higher than 700°C, indicates a change in anode reaction mechanism.

4) Initial anode polarization is capacitive in nature and is due to a double layer charge distribution. Up to 75 percent of the steady state polarization can be attributed to capacitive discharge at 600°C.

5) The proposed two step anode reaction incorporating the initial Boudard shift and subsequent electrochemical oxidation of carbon monoxide to carbon dioxide should be further critically tested. A proposed method of testing this two step process is to determine the effect of compounds, which are known to promote the Boudard reaction (e.g. iron oxide), on the anode reaction. Other methods of catalyzing the anode reaction should also be investigated, e.g., the determination of the effect of depositing various noble metals as silver, gold, platinum, and palladium upon the anode polarization. It seems plausible that the metal to semiconductor contact would create an activated region in the graphite that is adjacent to a metal deposit. A necessary requirement for successful catalysis, according to the above suggested model, is that the work function of the metal be greater than that of the graphite.

BIBLIOGRAPHY

1) Adams, A. M. Fuel cells. Chemical and Process Engineering 35:199-203. 1954.

2) Baur, Emil and H. Ehrenberg. Über neue Brennstoffketten. Zeitschrift für Elektrochemie 22:1002-11. 1912.

3) Baur, Emil, Agnes Peterson and G. Füllemann. Über Brennstoffketten bei hoher Temperature. Zeitschrift für Elektrochemie 22:409-414. 1916

4) Baur, Emil and H. Preiss. Abhandlungen Brennstoffketten mit Festleitem. Zeitschrift für Elektrochemie 44:695-698. 1938.

5) Baur, Emil and Jakob Töbler. Sammelreferat Brennstoffketten. Zeitschrift für Elektrochemie 39:169-80. 1933.

6) Baur, Emil, W. D. Treadwell and G. Trümpler. Ausführungsformen von Brennstoffketten bei hoher Temperatur. Zeitschrift für Elektrochemie 27:199-209. 1921.

7) Becquerel, A. C. Treatise on electricity in: McKee, J. H. and A. M. Adams' Production of electricity from coal. Fuel 28:1-6. 1949.

8) Broers, Gerard H. J. High temperature galvanic fuel cells. Ph. D. thesis. University of Amsterdam, 1958. 314 numb. leaves.

9) Chambers, H. H. and A. D. S. Tantram. Carbonaceous Fuel Cells. in: G. J. Young (Ed.) Fuel Cells. New York, Reinhold, 1960. p. 94.

10) Delahay, Paul and Charles W. Tobias (eds). Advances in electrochemistry and electrochemical engineering. New York, Interscience 1961, 2 vols.

11) Drossback P. et al. Anodenprozesse bei der Elektrolyse geschmolzener Salze. Chemie Ingenieur Technik 33:84-91. 1961.

12) Gorin E. and H. L. Recht. Fuel cells. Chemical Engineering Progress 55: 51-9. August 1959.

13) Grove, William R. On the voltaic series and the combustion of gases by platinum in: A. M. Adams' Fuel cells. Chemical and Process Engineering 35:199-203. 1954.

14) Haber, F. and L. Bruner. Das Kohlenelement, eine Knallgaskette. Zeitschrift für Elektrochemie 10:697-713. 1904.

15) Howard, H. C. Direct generation of electricity from coal and gas. in: H. H. Lowry (ed.) Chemistry of coal utilization. Vol. 2 New York, John Wiley and Sons. 1945. p. 1586.

16) Howarth, J. T. and W. E. I. Turner. Decomposition of sodium carbonate by heat. Journal of the Society of Glass Technology 14: 394-401. 1930.

17) Ives, David J. G. and George J. Janz (eds.). Reference electrodes, theory and practice. New York, Academic Press, 1961. 651 p.

18) Janz, George J. and Francisco Colom. Oxygen overpotential in molten carbonates. Troy. N. Y., Rensselaer Polytechnic Institute, 1959. 10 p. (U. S. Dept. Commerce, Office of Technical Services. P. B. Report 148, 566)

19) Janz, George J. and Max R. Lorenz. Molten carbonate electrolytes: physical properties, structure and mechanism of electrical conductance. Journal of the Electrochemical Society 108:1052-57. 1961.

20) Janz, George J. and Fumihiko Saegusa. Molten carbonates as electrolytes: viscosity and transport numbers. Journal of the Electrochemical Society 110:452-6. 1963.

21) Janz, George J. and Fumihiko Saegusa. Oxygen electrode in fused electrolytes. Electrochimica Acta 7:393-8. 1962.

22) Justi, Edward, Kurt Bischoff and Herbert Spengler. Stand und Aussichten der reversiblen Erzeugung elektrischer Energie aus festen Brennstoffen in Brenstoffelement mit festem Elektrolyten. Akademie der Wissenschaften und der Literatur, Mainz. Mathematisch-Naturwissenschaftliche Klasse. Abhandlungen, 1956. p. 3-26.

23) Kortüm, G. and J. O'M. Bockris. Textbook of electrochemistry New York, Elsevier, 1951. 2 Vols.

24) Kröger, Carl and Ernst Fingas. Die Einwirkung von Quarz und Alkalisilikaten auf alkalicarbonate. Zeitschrift für Anorganische und Allgemeine Chemie 213:12-57. 1933.

25) Mckee, J. H. and A. M. Adams. Production of electricity from coal. Fuel 28:1-6. 1949.

26) Potter, Edmund C. Electrochemistry principles and applications. London, Cleaver-Hume Press Ltd., 1956. 418 p.

27) Rideal, Eric. On fuel cells. Zeitschrift für Electrochemie 62:325-7. 1958.

28) Smith, J. M. and H. C. Van Ness. Introduction to chemical engineering thermodynamics. 2d ed. New York, McGraw Hill, 1959. 490 p.

29) Spengler, H. Brennstoffelemente. Angewandte Chemie 68: 689-92. 1956.

30) Taitelbaum, I. Studien über Brennstoffketten. Zeitschrift für Electrochemie 16:286-300. 1910.

31) Tamaru, Setsuro and Monoru Kamada. Brennstoffketten, deren Arbeitstemperatur unterhalb 600°C liegt. Zeitschrift für Elektrochemie und Angewandte Physikalische chemie 41:93-6. 1935.

32) Wicks, Charles E. and Frank E. Block. Thermodynamic properties of 65 elements their oxides, halides, carbides, and nitrides. 1963. 493 p. (U. S. Bureau of Mines. Bulletin 605)

33) Young, G. J. ed. Fuel cells. New York, Reinhold, 1960. 154 p.

APPENDIX

APPENDIX

"On the Current Carrying Capacity of the Platinum Wire Reference Electrode"

As indicated in Chapter III, a platinum wire electrode used as the anode reference electrode was subjected to a small current flow during polarization measurements owing to the recorder input impedance of 100,000 ohms.

An experiment was conducted in which two identical smooth platinum wire electrodes were immersed in a eutectic mixture of the fused carbonate electrolyte. Current was passed between the wires in both the forward and reverse direction and induced potentials between the electrodes were measured. Several cycles of increasing and decreasing current were recorded to determine if a permanent electrode potential would be observed when the current was returned to zero. The results of one series of experiments are presented graphically in Fig. 18. Other temperatures were studied, but the results depicted in Fig. 18 are typical in that the open circuit potential always returned to within five millivolts of zero. The electrolyte was saturated with carbon dioxide and oxygen by bubbling in an equimolar mixture of the gases.

As seen from Fig. 18, there is negligible effect on the open circuit potential between the two platinum wires after a cycle of increasing and decreasing the current flowing through the system for

both forward and reverse currents. At 640°C, the potential between both electrodes is approximately three millivolts per 0.01 milliamps. The polarization may be assumed to be equally divided between each electrode, so a 0.01 ma/cm^2 current density at a point reference electrode results in only a two millivolt polarization at 640°C. Reference electrode polarization is further reduced for higher temperature operation.

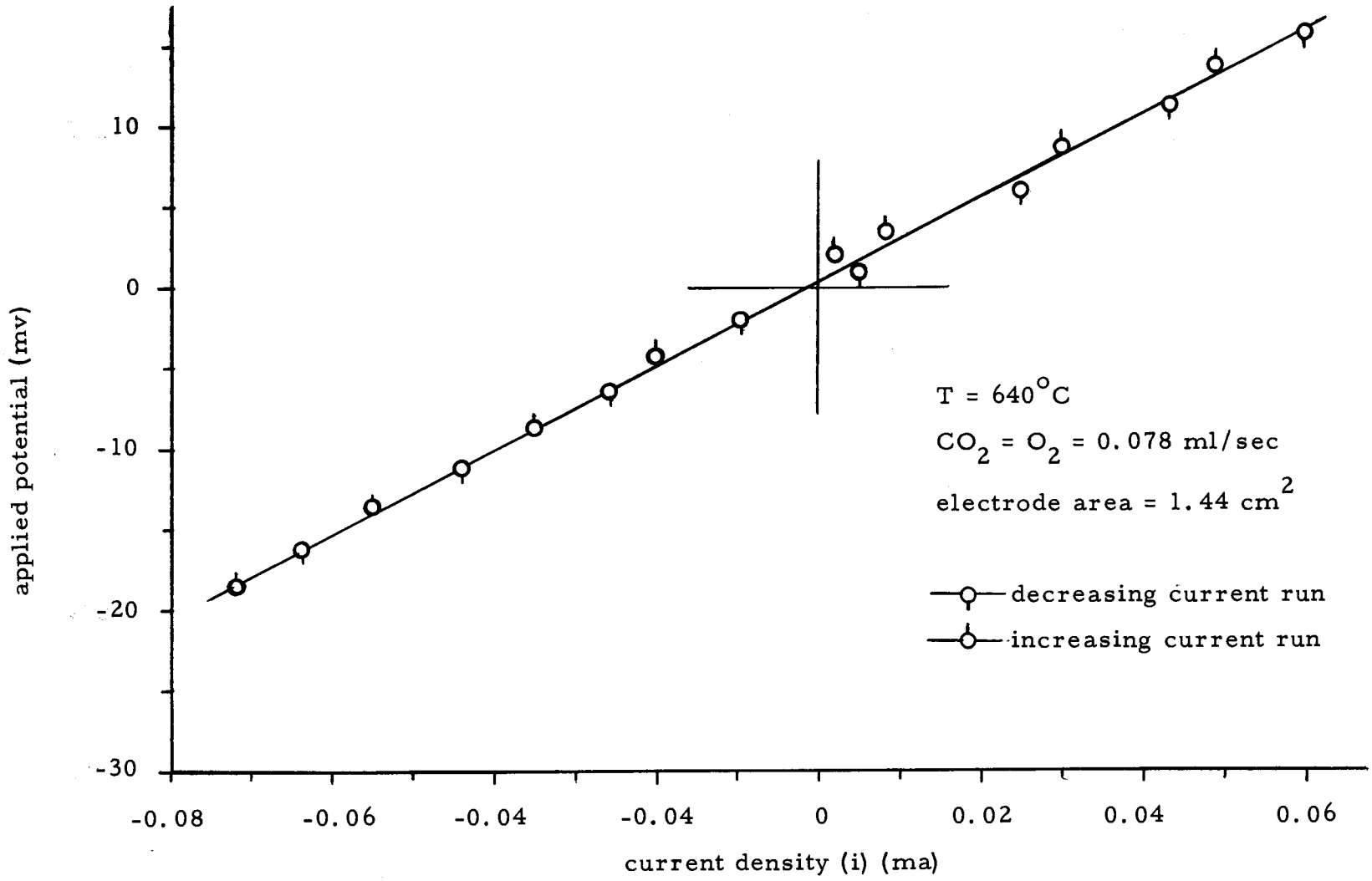

Fig. 18. Polarization of smooth wire electrodes.

NOMENCLATURE

Symbol	Definition
a	Thermodynamic activity
$\bar{d}$	Length vector
e	Electron
i	Current density
k	Reaction rate constant
n	Number of electrons transferred per molecule
r	Anode gas generation rate
t	Time
A	Surface area of anode
C	Electrical capacitance
E	Electric potential
$\bar{E}$	Electric field vector
F	The Faraday
P	Pressure
R	Gas constant
S	Entropy
T	Temperature
U	Activation energy of electrochemical reaction

Greek Letters

α	Transfer number

Symbol	Definition
β	A proportionality constant defined on page 45.
η	Anode polarization
Δ	Change in quantity

Subscripts

A	Component A
d	Decomposition
o.c.	Open circuit
s	Saturated
( )	Subscripted quantity refers to the equation number between the parenthesis

Superscripts

o	Thermodynamic standard reference state